1999

A windtunnel study of thin-sheet and rivulet icing formation on planar surfaces

Jeffrey Thomas Streitz Jr
University of Iowa

A WINDTUNNEL STUDY OF THIN-SHEET AND RIVULET

ICING FORMATION ON PLANAR SURFACES

by

Jeffrey Thomas Streitz Jr.

A thesis submitted in partial fulfillment of the requirements for the
Master of Science degree in Civil and Environmental Engineering
in the Graduate College of The University of Iowa

May 1999

Thesis supervisor: Professor Robert Ettema

Graduate College
The University of Iowa
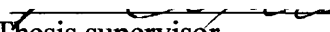Iowa City, Iowa
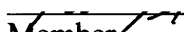
CERTIFICATE OF APPROVAL

MASTER'S THESIS

This is to certify that the Master's thesis of

Jeffrey Thomas Streitz Jr.

has been approved by the Examining Committee for the thesis requirement for the Master of Science degree in Civil and Environmental Engineering at the May 1999 graduation.

Thesis committee:

_____
Thesis supervisor

_____
Member

_____
Member

ABSTRACT

This thesis describes the design, development, and preliminary use of a unique icing windtunnel. A major objective of the study was to develop a windtunnel that would allow the investigators to study the influence of slope and wind on icing formations formed from thin films of water and water rivulets. A second objective was to present early findings, from the windtunnel experiments, on the initial formation of icings on planar surfaces.

The open-jet, tilting windtunnel developed for the present study is located in a refrigerated laboratory at the Iowa Institute of Hydraulic Research. The windtunnel enables investigation of the influences of gravity and wind drag on the freezing of thin-sheet and rivulet flows of water. It does so by means of tilting the windtunnel test section and varying wind speed. The conditions investigated include those produced by variations in slope of inclined plane, windspeed, air and base plane temperature, and water-discharge rate.

The influences of slope and wind speed are found to significantly affect the surface topology of planar icing formations, the rate of spreading and thickening, and the resultant crystal structure. Distinct features of the various types of icings are documented, and are presented herein. The experiments showed that base slope and windspeed significantly affected icing morphology for thin-sheet and rivulet flow on

an aluminum surface. However, icings formed on an ice surface varied insignificantly with base slope and wind.

TABLE OF CONTENTS

LIST OF TABLES

LIST OF FIGURES

CHAPTER I

INTRODUCTION

This thesis presents findings from experiments investigating the icing of sloped planar surfaces exposed to wind. The experiments were carried out using an open-jet tilting windtunnel, developed especially for this study. The windtunnel is located in a refrigerated laboratory. It was used to extend earlier research conducted at the Iowa Institute of Hydraulic Research (Schohl and Ettema 1986) on planar icing formation.

The windtunnel facilitates investigation of the effects on icing formation of gravity and wind drag, which it enables by means of tilting the test section and varying wind speed. To varying extents, both gravity and wind drag may drive the spreading of shallow flows of freezing water introduced at the upstream end of the windtunnel test section. The conditions investigated include those produced by variations in slope of inclined plane, air temperature, water-discharge rate, and type of flow (sheet or rivulet) of the water over the planar surface on which icing forms. Developing the various components of the icing facility, including the windtunnel, was a major part of the work performed for the present study. Many design iterations were performed before arriving at the final design. Delivery of liquid water at a

controlled rate and temperature, in the freezing environment, proved to be particularly difficult.

Initial formation herein is defined as the initial, or foundation, layer of icing formed when shallow water first flows as a laminar sheet or rivulet over a frigid surface and freezes to it. Subsequent formation of icing is a continuing, cyclic process whereby thin layers of slush ice form and eventually freeze solid as irregular laminations that extend the area covered by the icing and thicken the icing formation.

Many variables affect icing formation from water flow as a thin sheet or rivulet on planar surfaces. The initial formation of such icing is the most sensitive stage of formation, because the most variables are at play. In particular, the variables characterizing the plane surface are influential. Once early layers of icing have formed, the number of influential variables decreases; e.g., heat flux to the base plane, plane slope, and plane roughness diminish in importance. Therefore, the initial spreading of planar icing is an important stage to investigate. It is of particular significance for icing of diverse surfaces, such as aircraft, automobiles, roads, and bridges.

No prior studies have been conducted on the freezing of thin sheets or rivulets. Schohl and Ettema studied sheet flow freezing on a nearly horizontal plane, but did not examine the freezing of sheet flow on a sloped surface. Nor did they consider the influence on icing characteristics of wind.

1.1   Objectives

The goals of the research findings reported herein were as follow:

1. To develop a purpose-designed icing windtunnel for the study of planar icing formation;

2. To obtain preliminary insight on the effects of wind and slope on planar icing formations developing from sheet flows.

3. To gain insight on the effects of wind and slope on planar icing formations developing from rivulet flows.

The first task of the study entailed designing and developing a workable icing windtunnel. The subsequent tasks were to conduct experiments on planar icing of sheet flow and rivulet flow. Icing formation on an aluminum surface covered with small, hemispherical ice bumps was studied to gain insight into a particular occurrence observed on aircraft wings. Aircraft icings often exhibit regions of bumpy ice formed from impinging water or rivulets or sheets that have broken up into water beads and subsequently frozen. Figure 1.1 illustrates areas on an aircraft wing at which diverse ice surface have been observed. One objective of the present study was to gain preliminary insight on how one such surface may affect icing topology.

Enlarged
View

Enlarged
View

?

?

Air/Water
Droplets
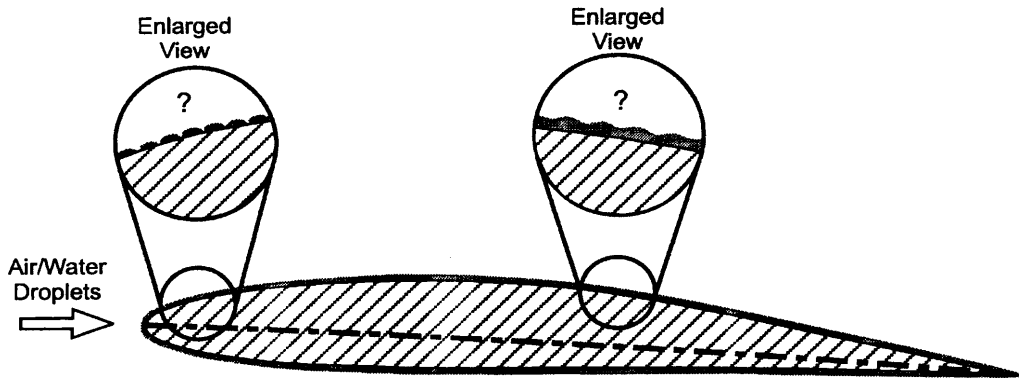
Figure 1.1   Regions of observed diverse iced surfaces on aircraft wings.

1.2   Thesis structure

Chapter II discusses common problems associated with planar icing formation. A survey of literature relevant to this study is also presented. Although not exhaustive, the literature review points out and discusses important topics related to the diverse problems associated with planar icing and supports the need for the research conducted in the present thesis, and for future research. Chapter III presents the experimental apparatus, an icing windtunnel, designed and constructed for this study. Photographs and drawings of the icing windtunnel and related equipment are given in this chapter. In Chapter IV, the experimental procedure is presented. Chapter V describes in detail the results obtained for planar icing cases of sheet and rivulet flow. Chapter VI presents the primary conclusions from the study and it offers recommendations for future research on planar surface icing.

CHAPTER II

BACKGROUND

Planar icings occur in many guises that vary in accordance with the nature of the base plane on which icings form, the rate of water supply, the ambient air and base surface temperatures, and the presence of wind. Their occurrences are rather common. Planar icing causes problems with diverse civil engineering structures (e.g. roadways, culverts, and spillways), as well as aircraft, automobiles, and ships.

2.1   Problems associated with planar icing

Icings cause many problems in natural drainage systems and on man-made structures in cold regions. When the necessary conditions for ice formation prevail, many different types of icing may form on a variety of base surfaces. These conditions often occur for parked or taxiing aircraft, for aircraft flying at relatively low elevations, and for stationary structures subject to wind. Icing concerns related to aircraft alone are justification for the study of planar icing, given the related safety issues.

A particular type of planar icing is of great concern in civil engineering drainage systems. Aufeis (originally German, a word meaning "on ice") is a spreading and thickening ice accretion that grows in cold regions when a shallow supply of water flows over a frigid surface (such as ground, concrete, or previous

ice cover) and freezes progressively to it. Initially, the water freezes directly to the surface over which it flows. Subsequent formation of aufeis occurs as a continuing, cyclic process whereby layers of slush ice form and eventually freeze solid as laminations that extend the area covered by the icing as well as thicken the icing formation.

Aufeis occurs in many situations that vary in accordance with existing conditions, and its occurrence is rather common. For example, it typically is found in shallow streams, rivers, and drainage courses, such as the roadside ditch depicted in Figure 2.1. It also occurs on roads, pavements, and on diverse other engineered structures. A variety of engineering problems arise from aufies development. Blockage of drainage facilities and the subsequent flooding are a major concern in cold regions. Furthermore, aufeis formations, also referred to as naleds (from Russian), may make roads, runways, railroads, tunnels, or mines impassable.

2.2   Literature review

An extensive literature review is not presented herein. A thorough overview of the literature on naled ice growth can be found in the paper by Schohl and Ettema (1986). Schmuki and Laso (1989) and Mizumura (1993) offer comprehensive reviews of rivulet stability. An overview of the literature on the primary instabilities of film flow is given by Liu et al. (1992). The ensuing review is a concise synopsis of published insights into icing formation on sloped surfaces. It contains brief reviews of aircraft icing, film flow, rivulet flow, and planar icing.

Figure 2.1   Aufeis formation in a drainage ditch.

2.2.1 Aircraft icing

Due to related safety matters, icing formation on wing, tail, and fuselage surfaces of aircraft is of great concern. Icing of aircraft wings results in a reduction of lift coefficient and stall speed, an increase in drag coefficient, and a relatively small increase in aircraft weight. Aerodynamic performance of aircraft hindered by ice formation has, therefore, been widely studied over the past decades.

If an aircraft wing leading edge is continuously heated, impinging water, even in frigid conditions, may stay in a liquid state and flow downstream where it could entirely or partially wet the wing surface, evaporate, or freeze. Alternatively, in the case where an aircraft wing is not continuously heated, impinging water may freeze upon impact and subsequently continue to build up on the surface until a de-icing mechanism is employed for ice shedding. If thermal means are used to de-ice the surface, water (melted ice from the wing/ice interface) can runback and possibly refreeze. This phenomenon is commonly referred to as the "runback" problem (e.g., see Al-Khalil et al. 1990).

Anderson et al. (1984), Hansman et al. (1989), Hansman and Turnock (1989), Al-Khalil et al. (1989, 1990, 1991, 1993), Rothmayer and Tsao (1998), and many others have significantly contributed to the understanding of icing arising from impingement and/or runback. The experiments in the present study examine the formation of ice, given water supplied by the aforementioned mechanisms, in the vicinity of the leading stagnation zone along a wing or tail section, where relatively low air speeds may develop.

2.2.2 Film flow

Thin liquid films flowing down inclined planar surfaces are common in engineering and natural processes. The driving forces of such flows include gravity, pressure gradients, moving boundaries, and shear stresses. Figure 2.2 depicts the forces usually acting on a liquid flowing down an inclined plane.
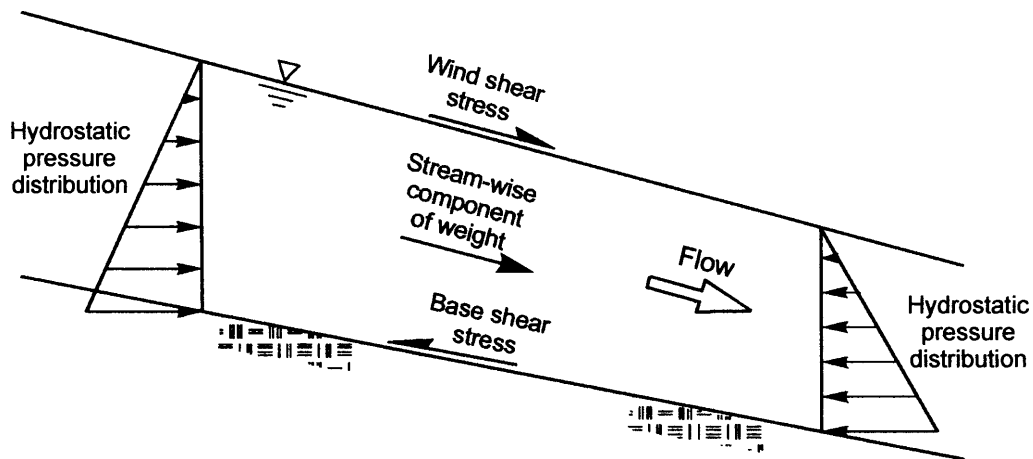
Figure 2.2   Forces on liquid flowing down an inclined plane.

A large amount of work has been performed on the flow of liquid over a plane as a film. The voluminous literature on the subject includes articles about systems that are isothermal, heated or cooled, composed of several liquid layers with density and/or viscosity stratification, and films that are contained within pipes or channels.

Film flows often exhibit instabilities evident as surface waves whose wavelength is much greater than the depth of the film. The stability of film flows has received extensive attention.   For example, Benjamin (1957) and Yih   ·

(1963,1967) performed pioneering theoretical work. Binnie (1957), Kao (1965a, b, 1968), Lin (1975), Akhtaruzzaman et al. (1978), Hickox (1971), Smith andDavis (1982), Joseph et al. (1984), Goussis and Kelly (1985, 1988, 1990), Hooper (1985), Renardy (1987a,b), Lister (1987), Than et al. (1987), Smith (1989,1990), and Liu et al. (1992), and many others have made significant contributions to the understanding of instabilities in film flow. No attempt here is made to summarize these studies, other than to say that film instability, and its origins, can be modeled very effectively these days.

The effect of heating or cooling the flow layer on the stability to the interface of long waves also has been investigated extensively. Results are reported in numerous papers. When Kelly and Goussis (1982) considered the problem, for example, they showed that buoyancy forces and direct liquid expansion could be neglected in the layer when the thermal expansion coefficient is small. They concluded that thermal effects do not significantly influence the characteristics of the long-wave instability in inclined layers. Smith (1990) showed that this result is only strictly true for liquid layers with small to moderate values of the Prandtl number. The Prandtl number is the ratio of the capacity of a fluid to diffuse momentum to its

capacity to diffuse heat. It may be expressed as

$$Pr = \frac{\mu\, c_p}{k} \qquad (1)$$

where k = thermal conductivity, c_p = specific heat, and μ = viscosity. The Prandtl number involves fluid properties only, not the length and velocity scales of flow.

The present study does not attempt to expand on the physics of thin film flows. The literature on this is already extensive. The study instead goes on to provide intriguing insights into the behavior of such flows under frigid conditions. The flows examined here exhibited both the bed-shear and wind shear induced waves effectively described by the references mentioned above.

2.2.3 Rivulet flow

The forces that drive rivulet flow are the same as those that drive film flows (Figure 2.2), except that surface tension plays an even more important role in rivulet formation and flow. The base surface on which rivulets flow is not entirely covered with water. Small streams (rivulets) of water trickle around dry patches of non-wetting surface. An important surface tension effect is the contact angle Θ that occurs when a liquid interface intersects with a solid surface, such as sketched in Figure 2.3. Surface roughness may also influence rivulet formation. Figure 2.3 shows a typical cross-section of a rivulet. When Θ is less than 90 degrees, the liquid is said to wet the solid. Conversely, when Θ is greater than 90 degrees, the liquid is termed non-wetting. For example, though water may wet a rough aluminum surface, rivulets form on smooth aluminum. If the contact angle were lower, it would be difficult to form rivulets, as the flow would just spread out very thin.
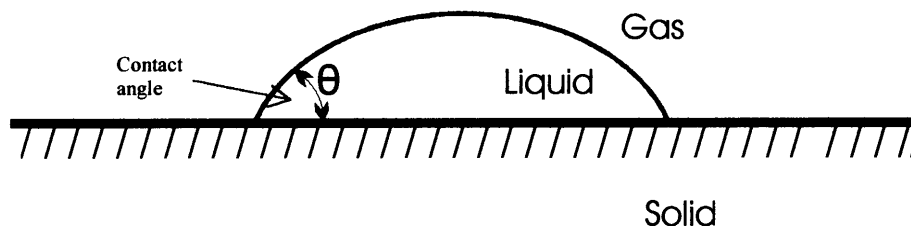
Figure 2.3   Example rivulet cross-section

Although the literature indicates that the most studied thin-flow regime is that of a film flowing down an inclined plane, rivulets have also received a significant amount of attention. A few example studies of note are as mentioned here. Towell and Rothfeld (1966), for instance, obtained the shape and velocity distribution of rivulets by comparing experimental results to the solution of the Navier-Stokes equations for the case of laminar flow. Gorycki (1973) concluded that helical flow in a water rivulet is important to rivulet meandering. Davis (1980) investigated liquid-solid interaction. Weiland and Davis (1981) studied instabilities of long waves formed in rivulets. Nakagowa and Scott (1982) determined that rivulet sinuosity increases with both discharge and base slope. Culkin and Davis (1984), Schmuki and Laso (1990), Mizumura (1993), and Mizumura and Yamasaka (1997) all furthered the understanding of the various flow regimes of rivulets. Typical rivulet –flow regimes are straight, sinuous, meandering, and branched.

The present study illuminates aspects of rivulet flow and subsequent ice development in frigid-air conditions.

2.2.4 Planar icing

The topic of icing formation on planar surfaces has received little rigorous investigative attention, largely due to the difficulty of developing it under controlled conditions. Icing literature (e.g., the major reviews conducted by Carey 1973, Slaughter 1990) completely lacks mention or illustration of the range of icing formations on planar surfaces or of the basic mechanisms by which it spreads and thickens. This deficiency in the literature is, perhaps, not surprising, as the required experimental facilities have not been available heretofore, with the exception of the similar, but more limited, apparatus developed by Schohl and Ettema (1986). Schohl and Ettema investigated icing formation on a smooth horizontal plane. Figure2.4 shows the experimental setup utilized by them. It comprises a manifold that release flow onto a flat frigid base.
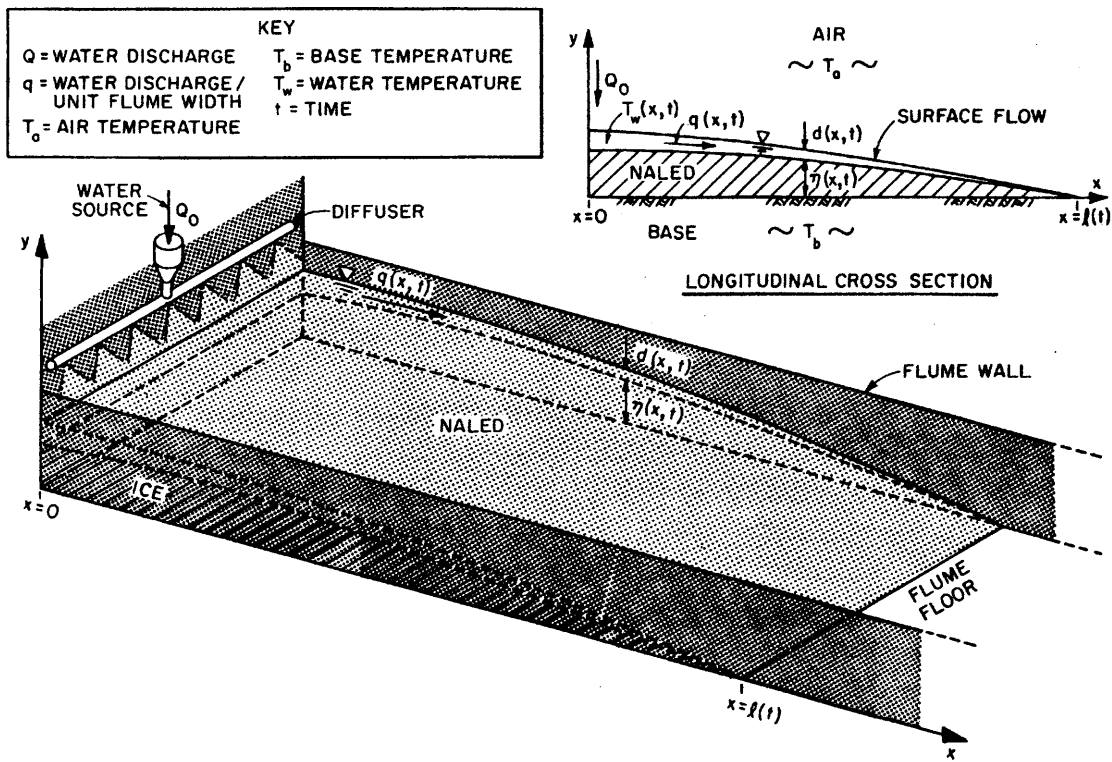
Figure 2.4   Experimental setup of Schohl and Ettema (1986).

The study by Schohl and Ettema was the first laboratory study explaining the processes associated with aufeis growth. The research before 1986 had been based primarily on visual observation, anecdotes, and field measurements. Schohl and Ettema found that the initial extent of spreading could be characterized using an equilibrium spread length l_e. The length l_e is an equilibrium length for which the volumetric rate of ice formation equals the volumetric rate of water supplied to the icing. It may be expressed as

$$l_e = \frac{q_o \rho_w L}{\Phi_{wa} + \Phi_p} \qquad (2)$$

The period associated with l_e is

$$t_e = \frac{l_e^2}{100 q_o} \qquad (3)$$

In equations (2) and (3), q_o = source-water discharge per unit width of icing, Φ_{wa} = heat flux to from icing to air, Φ_p = heat flux to/from plane, ρ_w and ρ_i = densities of water and ice, and L = latent heat of fusion for water.

The processes associated with the formation of the initial layer of icing are usefully described in terms of l_e and t_e. However, these variables do not include the effects of plane slope, planar roughness, or wind. Schohl and Ettema (1986) investigated icing formation on a nearly horizontal plane of ice. The ice plane replicated an ice cover on a shallow river. Icings may, of course, form on a variety of planar surfaces besides ice. In addition, the surfaces may be variably inclined and subject to wind.

The present study extends the laboratory study conducted by Schohl and Ettema (1986) by examining the influences on planar icing formation of plane slope, wind, and to a lesser extent planar roughness.

2.3   Important parameters

Consideration of the flow and heat transfer processes associated with thin-film

or rivulet freezing suggest that the important variables are as depicted in figure 2.5.
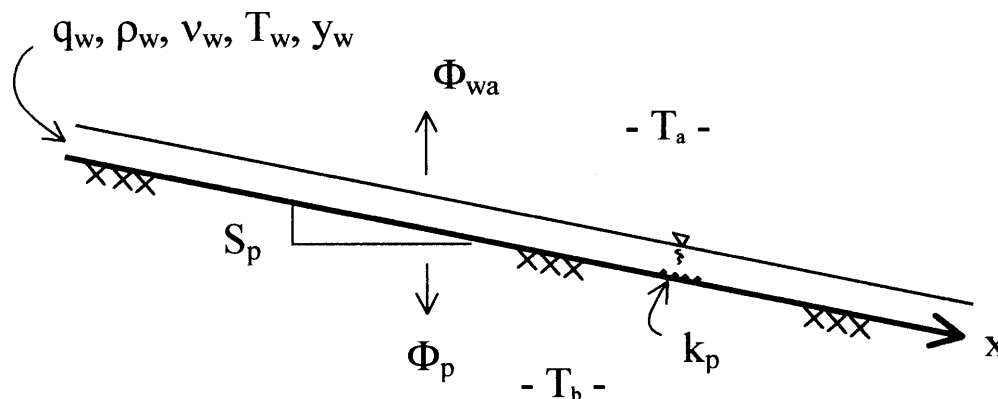
Figure 2.5   Variables associated with freezing of a water film on a sloped surface.

To describe icing formation on sloped planes, it is necessary to begin with, and

extend, the set of non-dimensional parameters identified by Schohl and Ettema for

describing icing on a smooth horizontal plane. It is necessary to introduce several

additional dependent variables for describing the state of icing formation. Those

dependent variables are overall thickness of icing, η, icing spread length, l, icing

roughness variables (spacing, λ_i, and height, k_i), porosity, p, water discharge per unit

width, q, and bond strength with base plane, τ_p. A dependent variable such as these,

generally is termed as A, and it depends on the set of independent variables given on

the top of the following page;

$$A = f_A\left(\eta, l, \lambda_i, \mathrm{k}_i, \mathrm{p}, \mathrm{q}, \tau_p, \mathrm{t}, \mathrm{S}_p, k_p, u_{*a}, \sigma, v_w, v_a, g, \alpha_w, \alpha_i, q_0, \Phi_{wa}, \Phi_p, \rho_w, \rho_i, L\right) \tag{4}$$

The variables in equation (4) may be expressed functionally in terms of a set of non-dimensional parameters;

$$\psi_A = \varphi_A\left(\frac{x}{l_e}, \frac{t}{t_e}, \frac{\Phi_{wa}}{\Phi_{wa} + \Phi_p}, \frac{\Phi_{wa}}{\rho_w L^{3/2}}, \frac{q_o}{v_w}, \frac{k_p}{Y_o}, \frac{q_o}{(gY^3)^{1/2}}, \frac{\alpha_i}{\alpha_w}, \frac{\rho Y_o q_o^2}{\sigma}, S_p, \frac{u_{*a} k_p}{v_a}\right) \tag{5}$$

In equations (4) and (5), ψ_A is a non-dimensional form of the dependent variable A, x = position along plane, t = time, S_p = plane slope, k_p = plane roughness, u_{*a} = an average value of shear velocity produced by wind over the plane, σ = surface tension between water and material comprising the base plane, v_w and v_a = kinematic viscosity of water and air, g = gravity acceleration, α_w and α_i = thermal diffusivity of water and ice, q_o = source-water discharge per unit width of icing, Φ_{wa} = heat flux to from icing to air, Φ_p = heat flux to/from plane, ρ_w and ρ_i = densities of water and ice, and L = latent heat of fusion for water.

Schohl and Ettema examined the influence of several of the first eight parameters in equation (5). The present study introduces and focuses on the last three parameters in equation (5). The parameters are Weber number $\rho Y_o q_o^2/\sigma$, plane slope S_p, and boundary Reynolds number for airflow over the plane $u_{*a} k_p/v_a$. Weber

number reflects the relative magnitudes of surface tension and inertia forces acting on a flow. The findings of the present study focus primarily on the effects on icing formation of the parameters S_p and $u_{*a}k_p/\nu_a$. The influence of Weber number is briefly considered. The other parameters in equation (5) were held constant for the study results presented here. In simple words, the study examines the influences of plane slope and wind speed on the initial formation of icing on an inclined plane.

CHAPTER III

THE ICING WINDTUNNEL

A significant portion of the effort for the present study entailed developing the various components of the icing windtunnel facility. A tiltable icing windtunnel was designed and assembled in 1997, and modified in 1998, in order to carry out the investigations described in this thesis. The windtunnel comprises an open-jet fan and a flow conditioning box located upstream of a planar aluminum test section. The whole windtunnel is mounted on a tiltable base, which can be inclined to an angle of about 15° down from the horizontal. In this manner, water may flow as a thin sheet or as rivulets propelled by wind drag and/or gravity. Many design iterations were performed before arriving at the final design discussed in this chapter. Difficulties dealing with the delivery of liquid water at a controlled rate and temperature in the freezing environment of the windtunnel test section spurred most of the design changes.

The icing windtunnel is located in a large refrigerated laboratory (lab) at the Iowa Institute of Hydraulic Research. Figure 3.1 shows the general layout of the lab and the icing windtunnel. The icing windtunnel sits in a concrete basin whose plan dimensions are 22.6 m by 4.8 m and a height of 3.0m.

El. -1.65m

TV Camera Trench
El. -1.0m

Icing Wind Tunnel

El. -1.65m

Ice Towing Tank
20 M x 5 M x 1.32 M Deep

Tank Wall

Main Floor El. 0.0m

0   5   10 Feet

0   1   2   3   4 Meters

PLAN VIEW OF ICE TOWING TANK
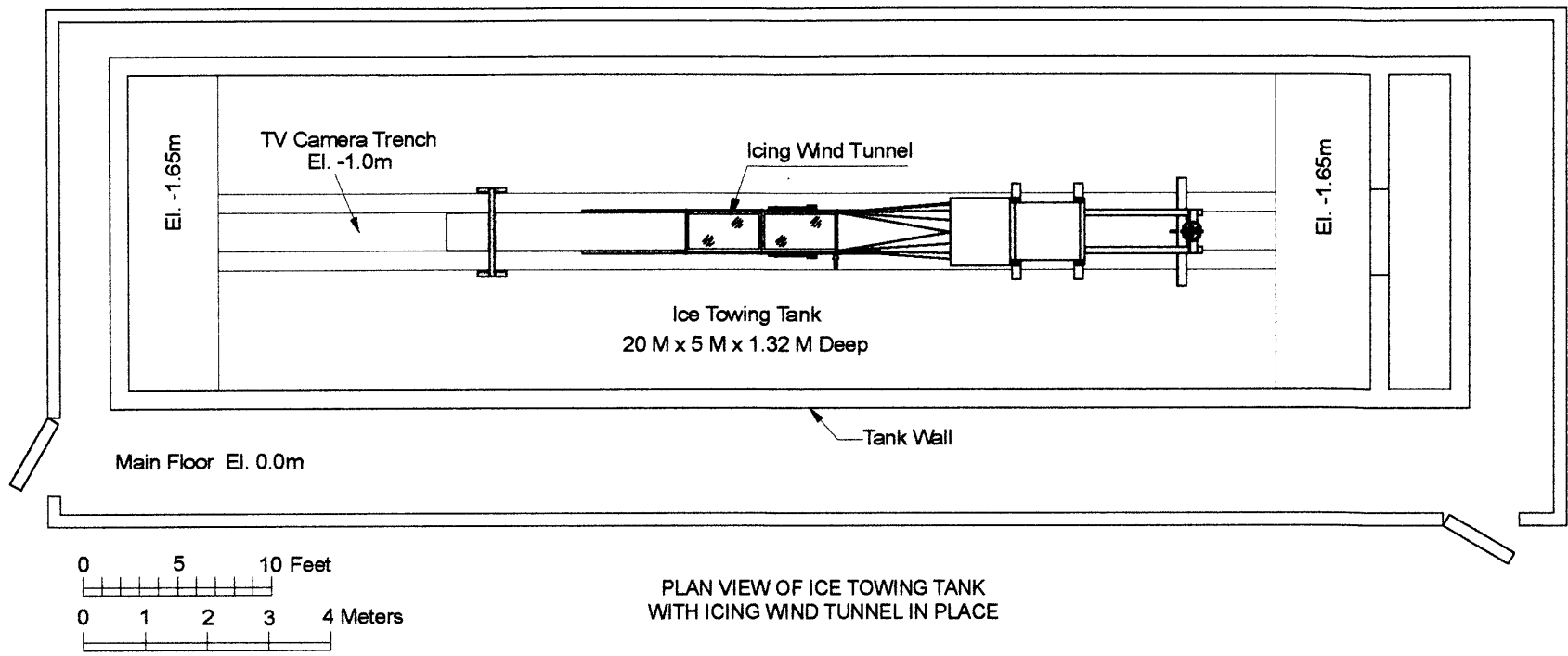WITH ICING WIND TUNNEL IN PLACE

Figure 3.1   Plan-view of refrigerated laboratory.

The air temperature in the lab is controllable, using thermostatically regulated evaporator units, to temperatures as low as -25°C, and can be computer-monitored by means of thermistors placed in a matrix of locations over each experimental set up. The lab is fitted with instrumentation for monitoring and recording air, water (inflow and along icing), and ice temperatures, water discharge, and icing thickness.

The fan produces wind velocities up to 83 km/hr, through a square test section 0.6 m wide by 0.6 m high. The velocity distribution was acceptably uniform across the test section. Figure 3.2 plots the velocity at two different points along the test section. The test section, made of 6.4-mm thick aluminum plate, was 2.4 m long for the laminar sheet-flow experiments and 6.3 m long for the rivulet-flow experiments. The first 2.4 m is enclosed with Plexiglas side and top walls.
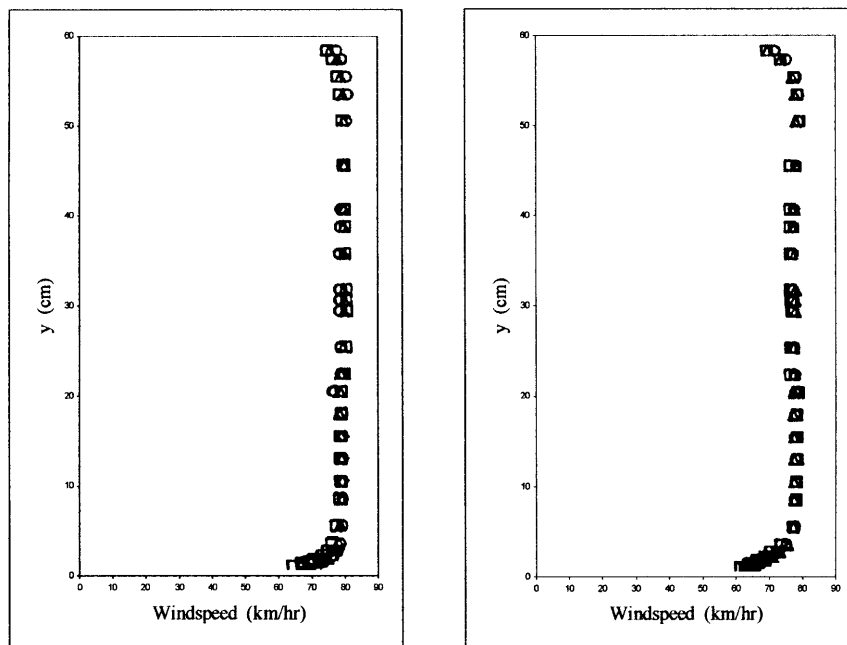
Figure 3.2   Velocity profiles in windtunnel test section. a) x = 0.9m   b) x = 1.9m
(x is positive in downstream direction with origin at the water inlet to test section)

A temperature-controlled manifold, attached to the base of the test section, was used to feed water to the upstream end through a row of 6-mm-diameter holes for the sheet-flow experiments, and a single 6-mm-diameter hole for the rivulet-flow experiments. Water flowed through insulated tubing to the manifold from a temperature- and flow-controllable chiller tank located outside of the refrigerated room. The manifold is fitted with a temperature gauge and heater to regulate the temperature of water fed into the test section. Water in the discharge manifold can be set at an initial temperature as low as $0.1^{\circ}C$ before being discharged over the aluminum plate of the test section. The temperature of the base is monitored by means of a thermistor. The overall layout and major dimensions of the icing windtunnel are shown in Figure 3.3.

Note that Figure 3.3 represents the icing windtunnel as configured for the sheet-flow experiments. The test section was extended to 6.3m for all rivulet experiments, as is illustrated in Figure 3.4.

PLAN VIEW OF ICING WIND TUNNEL IN PLACE ABOVE TRENCH

END VIEW

SIDE VIEW
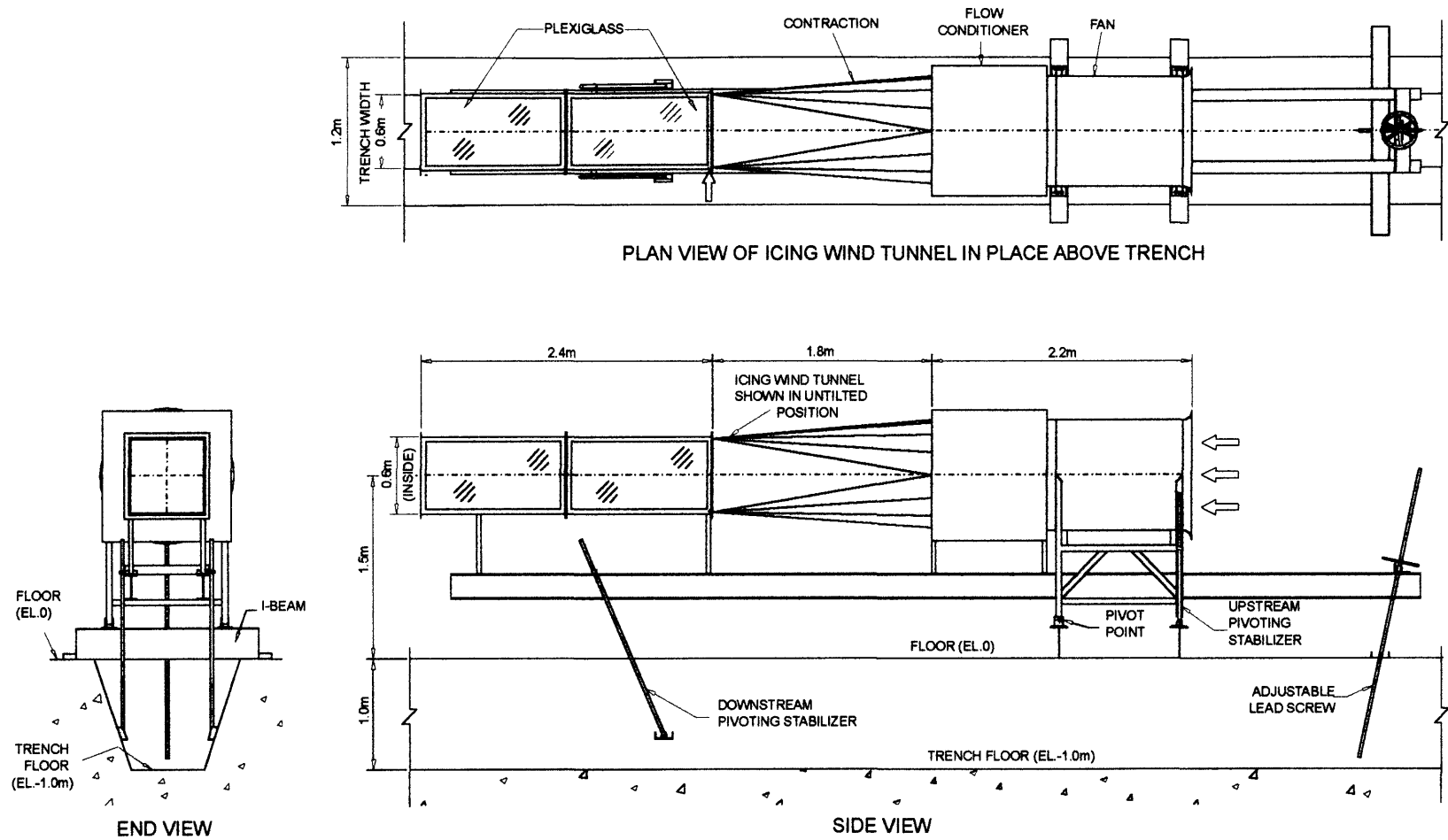
Figure 3.3   Layout of the tiltable icing windtunnel.

PLAN VIEW OF ICING WIND TUNNEL IN PLACE ABOVE TRENCH
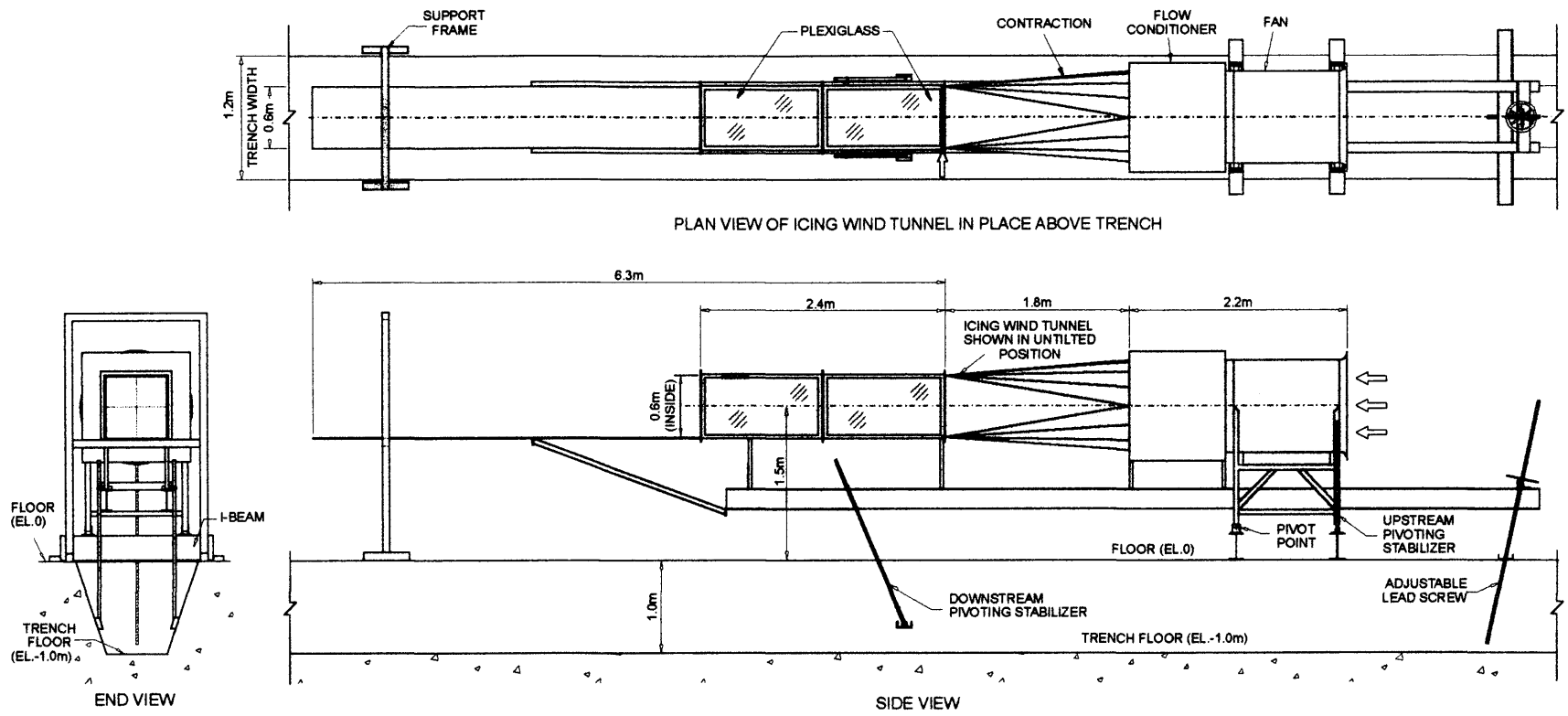
END VIEW

SIDE VIEW

Figure 3.4   Layout of the icing windtunnel as configured for rivulet experiments.

Any water flowing over the test section, and that does not freeze, is collected in a trough at the end of the test section. Figure 3.5, a diagram of the experimental setup, shows the flow path of the water. The chilled reservoir was located outside of the refrigerated room to enable the supply of water to the chilled reservoir to flow without freezing problems. A float-controlled valve let the water-surface elevation in the chilled reservoir be fixed and remain constant throughout the experiments. A fine-adjustable needle valve enabled the experimenters to accurately set the requisite flow rate. The tubing used to supply the chilled water to the test section was wrapped in foam insulation. Delivering a steady flow of liquid water to the upstream end of the test section proved to be particularly challenging. Many design iterations were performed before problems related to freezing in the tubing, and at the inlet to the test section, were subjugated. The solution required the use of the right amount of insulation to assure dependable water delivery at the required temperature of 0.1 degrees Celsius at the inlet to the test section.
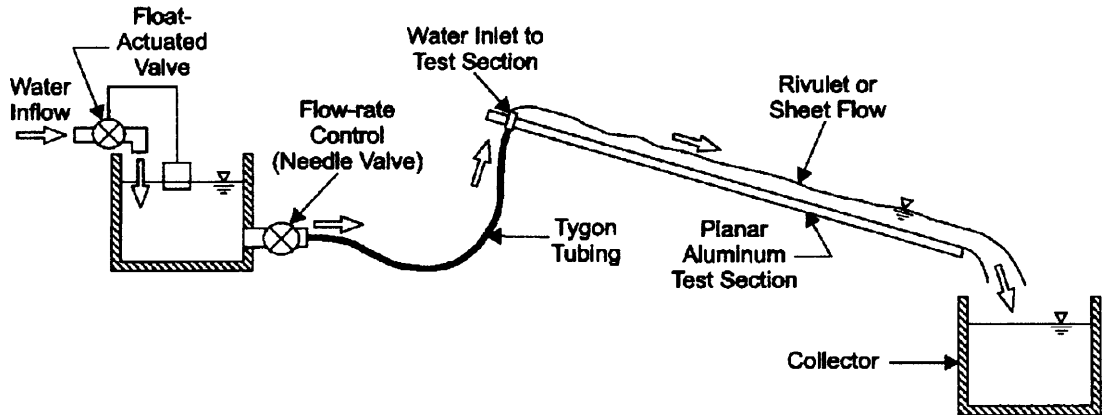

Figure 3.5   Diagram of water flow path.

The two optional mechanisms for driving the flow of sheets and rivulets of water (wind, gravity) enable the icing windtunnel to replicate the following component processes associated with icing formation on diverse planar surfaces:

1. Freezing of wind-drag driven flow of water discharged from a line or point source;

2. Freezing of gravity driven flow of water discharged from a line or point source; and,

3. Freezing of wind-drag and gravity driven flow of water from a line or point source.

Photographs of the icing windtunnel from various angles are presented in Figures 3.6 and 3.7. Note that the photographs in Figure 3.6 illustrate the icing windtunnel as configured for the sheet flow experiments, whereas those in Figure 3.7 depict it as set up for the rivulet icing experiments. Photograph 3.6a shows the icing windtunnel in the horizontal position. The following individual components of the windtunnel can be seen from left to right:

1. Fan assembly;

2. Flow conditioner;

3. Transition from the circular fan cross-section to the rectangular test section; and,

4. Test section.

The two I-shaped beams supporting the windtunnel are free to pivot about a point just under the downwind side of the fan assembly.

Photograph 3.6b depicts the icing windtunnel in an inclined position. The downstream end of the test section is allowed to pivot into a trough in the floor of the refrigerated room to a maximum of 15 degrees from the horizontal. Photograph 3.6c depicts the fan assembly and the slope adjustment mechanism. The slope of the icing windtunnel is adjusted by turning the wheel, which rides on a threaded lead screw passing through the cantilevered I-shaped beams. A system of jacks placed along the length of the windtunnel was considered but the simple lead-screw slope adjustment mechanism shown in the photos proved to be very stable and easy to construct. Photograph 3.6d shows the manifold outlet from which the water flows onto the planar surface of the test section. The manifold comprised a series of 6-mm-diameter holes spaced to produce sheet-flow along the test section. Considerable testing was performed to determine the optimum size and spacing of the holes. In the first design, water flowed from a slot in the manifold, but the setup proved to be too sensitive to level. The series of holes allowed surface tension to pull the water up to the test section inlet. A single 6-mm-diameter hole was used as the flow outlet for the rivulet experiments. The hole was placed centrally near the upstream end of the test section. The single 6-mm-diameter hole was simply the center hole of the series of holes used for the sheet flow experiments.

The test section was extended for all rivulet-flow experiments. Figure 3.7 shows two views of the icing windtunnel as configured for the rivulet-flow experiments. The point at which additional aluminum plate was extended can be seen in photograph 3.7a. Photograph 3.7b shows the support mechanism used to carry the additional 3.9 meters.

Figure 3.6   Photos of the icing windtunnel configured for sheet-flow experiments.

Figure 3.7   Photos of the icing windtunnel configured for rivulet-flow experiments.

CHAPTER IV

EXPERIMENTAL PROCEDURES

4.1   Sheet flow

Variations in planar icing topology for sheet flows were investigated in three series of experiments. All the experiments were performed with the unit water-flow rate held constant at 2.8 liters/min/m width and an initial water temperature of 0.1°C at the inlet to the test section. This discharge was chosen because it was the minimum flow rate required to produce a full sheet of water flow over the test section. The ambient temperature of the air and the base was –5°C. The three series of experiments were conducted with-

1. the base plane wetted immediately prior to starting an experiment, thus simulating the initial conditions of icing formation on a wet aluminum surface exposed to frigid air;

2. the base plane comprising a smooth ice base which was formed on the aluminum plate prior to the introduction of water; and,

3. the base plane covered with hemispherical bumps of ice on the aluminum plate prior to the introduction of water.

The aluminum surface was prepared for the smooth ice experiments by misting water onto the surface and allowing it to freeze. Successive applications

resulted in a smooth ice cover approximately 2mm thick. The hemispherical bumps were formed by dipping a board covered with regularly spaced nails into water then placing the board on the surface, allowing each nail head to deposit a single water drop. The average diameter of the bumps was 3.5 mm. Aerial density was 3 hemispherical bumps per square cm. The bumpy surface is shown in figure 4.1. The bumps were approximately similar to bumps reported for aircraft wings. However, the bumps were slightly larger in size.
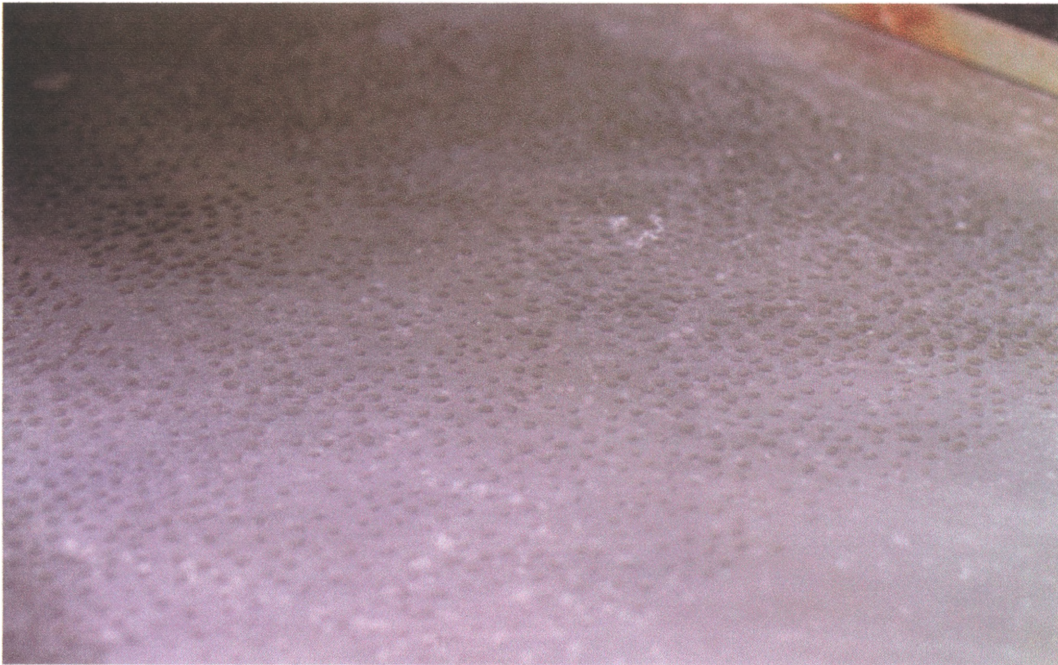

Figure 4.1   Hemispherical ice bumps on the aluminum surface of the test section.

4.2   Rivulet flow

To investigate variations in planar icing topology produced by rivulet flow, experiments were conducted with a water flow rate of 0.4-liters/min flowing from a single point source of 6-mm diameter at the upstream end of the test section. The test section was lengthened to 6.3 m for the series of experiments in order to allow observations of more fully-developed planar icing phenomena. The incoming water temperature was held constant at $0.1^{\circ}C$. The ambient temperature was held at $-9^{\circ}C$. As in the sheet flow cases, the flow was laterally constrained by the test section width of 0.6 m. The base plane was not wetted prior to starting an experiment, as in the sheet flow cases. Consequently, rivulets formed immediately at the source hole and propagated downstream. The experiments effectively simulated icing formation given the initial conditions of a dry aluminum surface in frigid weather, with water discharging from one or more source(s). It also replicated, though more loosely, rivulet formation from a sheet flow that has broken up into rivulets.

CHAPTER V

EXPERIMENTAL RESULTS

This chapter presents and discusses results obtained from experiments for the conditions of sheet-flow and rivulet-flow freezing. The results provide qualitative information on the morphologic characteristics and structure of icings.

5.1   Formation and typical features of sheet-flow icings on aluminum surface

Figure 5.1 is a sequence of sketches indicating how the initial layer of icing typically formed from sheet flow over an aluminum plane set at a mild slope and exposed to slight wind. The first ice crystals observed comprised small ice spicules attached to the plane. The ice formation began at and beyond approximately 1m downstream from the inlet to the test section. The ice formations progressed upstream to within approximately 20 cm from the water inlet to the test section. The spicules developed from fine (microscopic) roughness elements on the plane (i.e. scratches, burs, oxidation, etc.). The spicules quickly evolved as ice-crystal dendrites oriented across the plane and normal to the flow direction. As they grew, the dendrites increased the hydraulic roughness of the plane and locally deepened, thereby pooling the flow. As they grew toward the water surface, the transverse dendrites evolved an ice structure something akin to a maze of mini dams. When they

reached the flow surface, the transverse dendrites curved upstream into the flow and

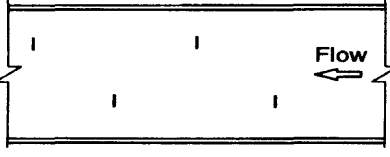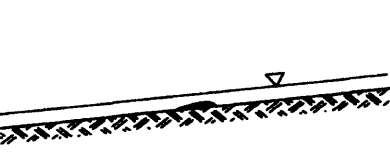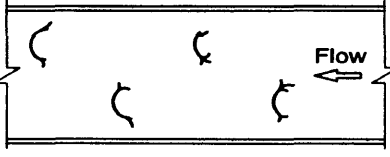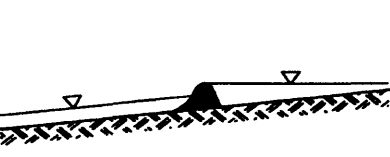bifurcated, the new dendrites creating additional mini-dams.
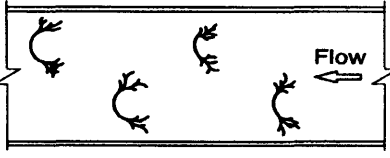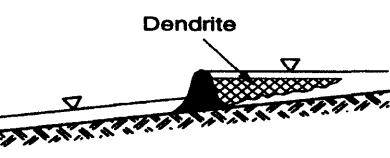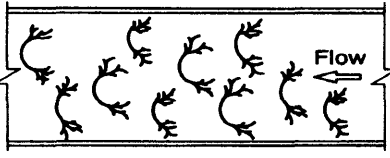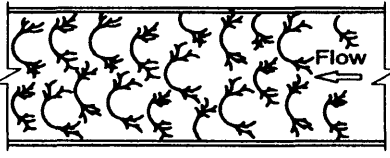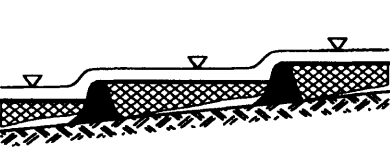
PLAN VIEW	CROSS-SECTION	COMMENTS
		Initial formation on plane disturbs flow. Ice spicules attach to plane.
		Height of disturbance increases as growth continues transversely and upstream. Pooling. Bifurcation.
	Dendrite	Continued growth of ice dam. Formation and growth of dendrites in pools. Direction of dendrite growth is unstream.
	Ice Cover	Surface ice-cover forms over locally pooled areas.
		Entire surface of icing freezes. Flow is forced over first layer.

Figure 5.1   Typical formation sequence for sheet-flow over an aluminum surface. The sketches show the main morphologic features associated with ice formation.

An intriguing feature of the first overall icing cover on the initially wetted surface is its choppy and wavy topology. As stated above, the initial icing resembled a three-dimensional array (or maze) of tiered mini-pools, each mini-pool retained by a mini-dam of ice. This appearance is significantly different than that of the icings observed by Schohl and Ettema (1986) forming on a horizontal plane of ice. Their icings were smoother (though not smooth) and quite different in ice-crystal structure than the icing depicted in Figure 5.2, a photograph of a typical formation for the median windspeed and slope. The scale of the features may be estimated by the distance between the screws in the upper-left portion of the photograph (16cm).

The icing shown in Figure 5.2 is typical. It was very porous and weakly bonded to the base plane. During the latter stage of its development, water trickled over and through the icing layer. Even after the free surface of the icing had frozen over, much of the icing layer remained unfrozen and became enveloped by an ice cover. The crystal structure of the icing was quite delicate. One could scratch a furrow through it with one's finger.

For icing formation on a wet aluminum base, plane slope and wind speed significantly influence icing surface features (topological variables, such as roughness height and spacing) and initial extent and rate of spreading. A qualitative discussion of the effects utilizing photographs ensues. A quantitative treatment of the same subject employing plots may be found later in this section.
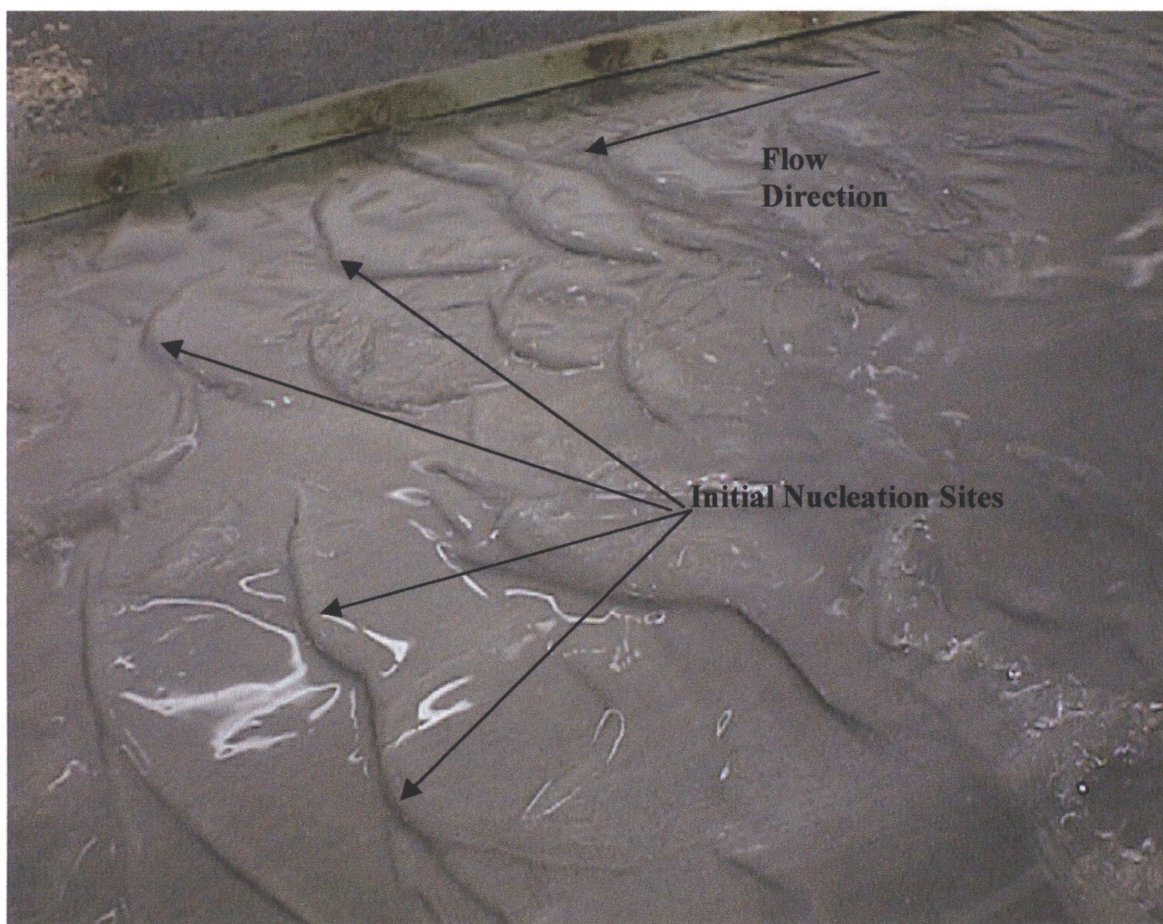
Figure 5.2   Typical features of sheet-flow icing forming on an aluminum surface.

A summary overview of the variation is evident in Figure 5.3, which presents a matrix of photographs illustrating the variations in icing topology observed for plane slopes up to $15°$ and wind speeds up to 48 km/hr. The matrix shows the appearance of the initial layer of icing formed for combinations of these variables. The aerial density of initial transverse dendrites and consequent mini-dams was

greater for the greater plane slopes and wind speeds. Hence, for a flat slope, dendrite formation resulted in longer mini-pools of locally retarded water. The spacing of icing roughness features corresponds directly to the aerial density of initial transverse dendrites. The greater height of the icing roughness features, for the larger slopes, corresponds to the deeper mini-pools formed by the dendrites. Note the similarity of the 1 degree base slope, 0 km/hr wind photo to that of the drainage ditch figure 2.1. Again, the scale of the features may be estimated by the distance between the screws along the left side of the photographs (16cm).

The plots in figure 5.4 show the influence of slope angle on the spacing and height of surface features (roughness) of the icings. The data are for a light wind of 16 km/hr. The lines with circles marking mean data points represents icings formed on the aluminum base. The bars show the range of values observed. The trends shown are intriguing and rather contrary to what might be expected from the literature on icing. As the water first flows over the plane, it accelerates due to gravity and thins. Therefore, it might be anticipated that the scale of ice-formation height would decrease with increased slope. Instead, as evident in Figure 5.4a, the average roughness feature height for the case of an initially wet plane increased with increasing slope, at least for the range of slopes investigated. It is probable that roughness height would attain a maximum with slope, and become smaller with steeper slopes. At the limiting condition of ice formation on a vertical plane, the ice surface is smooth. At the other extreme of a horizontal plane, the roughness is much reduced.
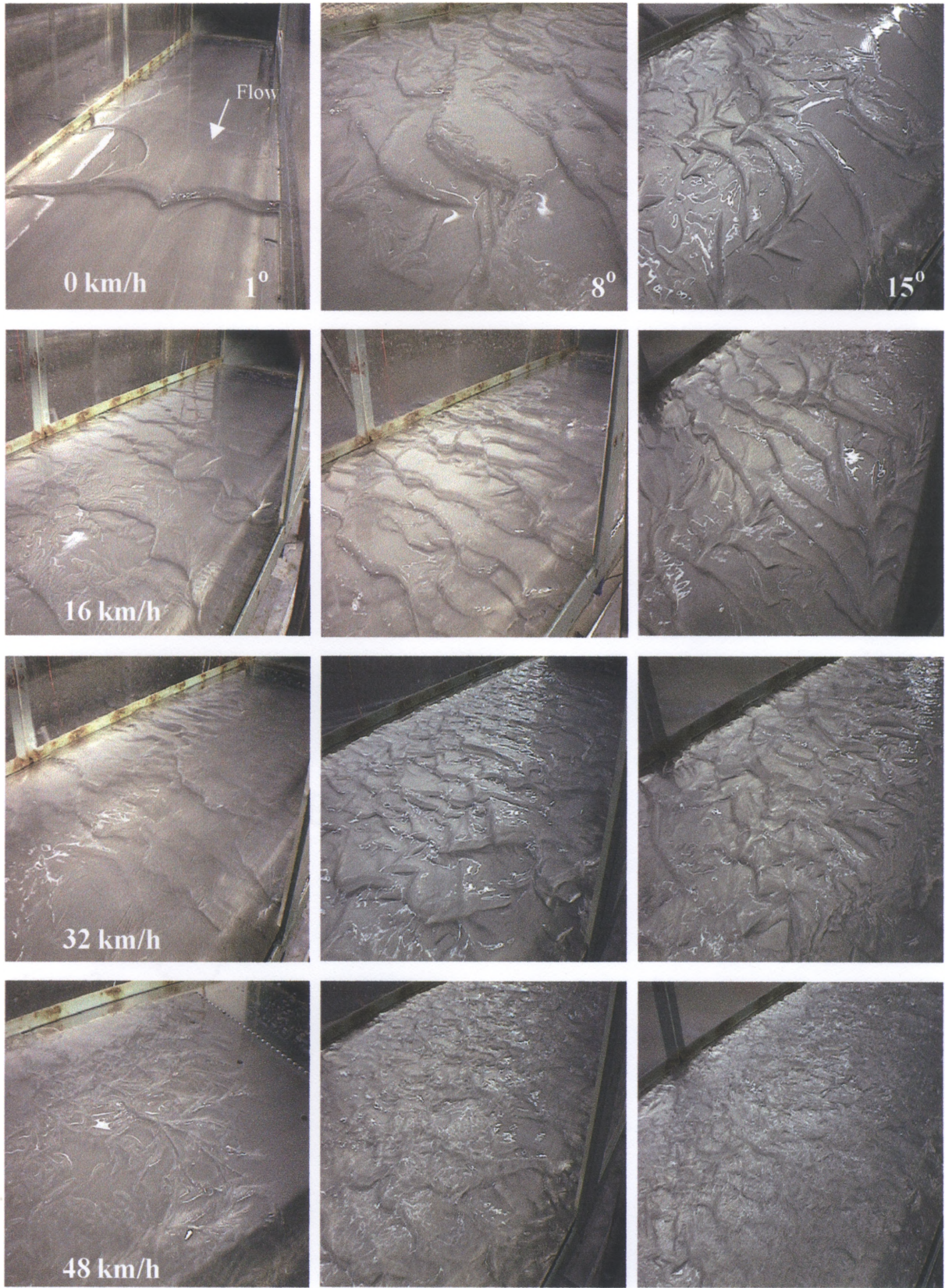
Figure 5.3   Topological variations of initial planar icing formed from sheet flow.

The trend shown in Figure 5.4b for roughness spacing, the average distance between distinct roughness features, indicates that it decreases with increasing slope of plane. It suggests that indeed the scale of surface features would decrease for planes at steep slopes. For plane slopes decreasing to a horizontal orientation, the roughness spacing essentially becomes the equilibrium length, l_e, as shown by Schohl and Ettema (1986). Increased slope caused the initial layer to spread and freeze further and faster. The aerial density of initial nucleation points increases with slope.

Figure 5.5 shows the effects of wind speed on surface roughness. Increased wind speed led to smoother icings. In other words, icing roughness spacing and height decreased with increasing wind speed, as can be seen in Figure 5.5. The trends are for a mild slope of $8°$.

Figure 5.4. Influence of plane slope on icing roughness (windspeed =16 km/hr)
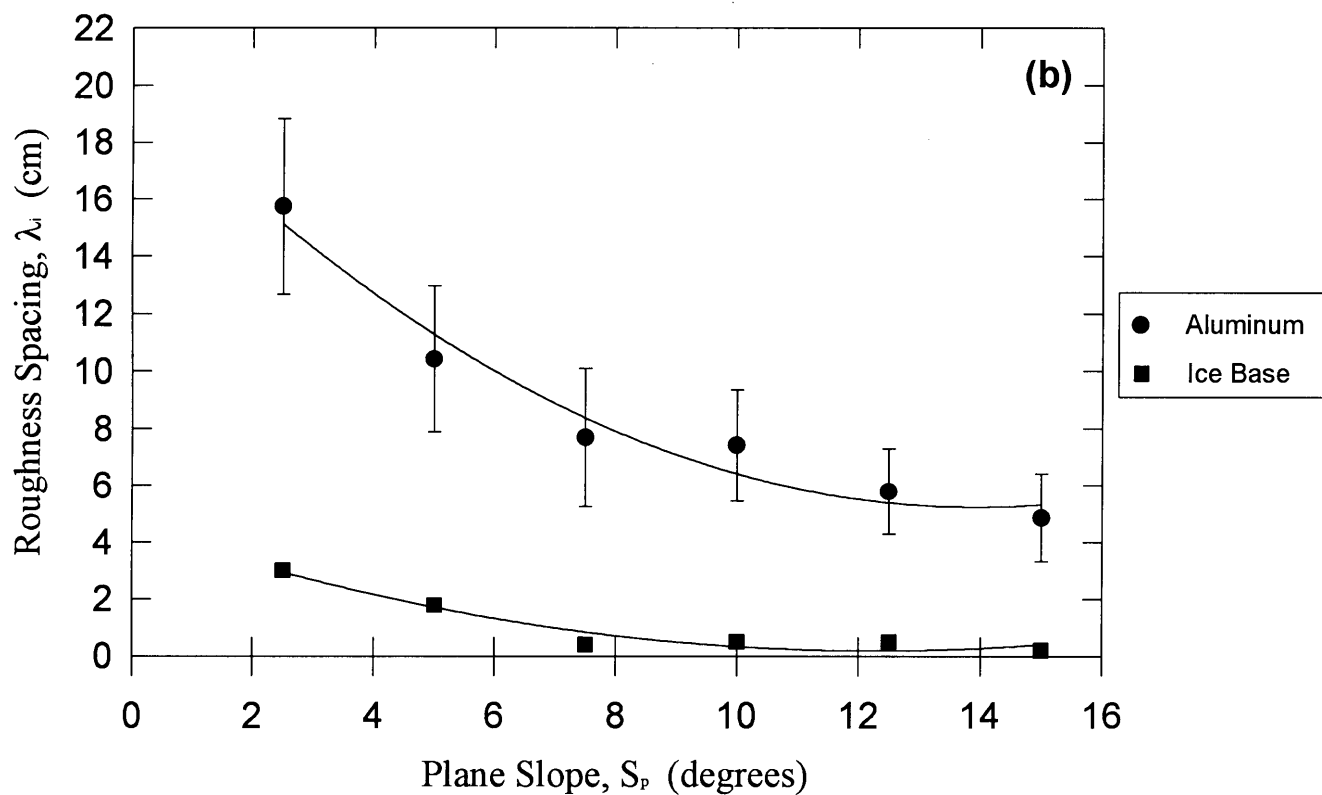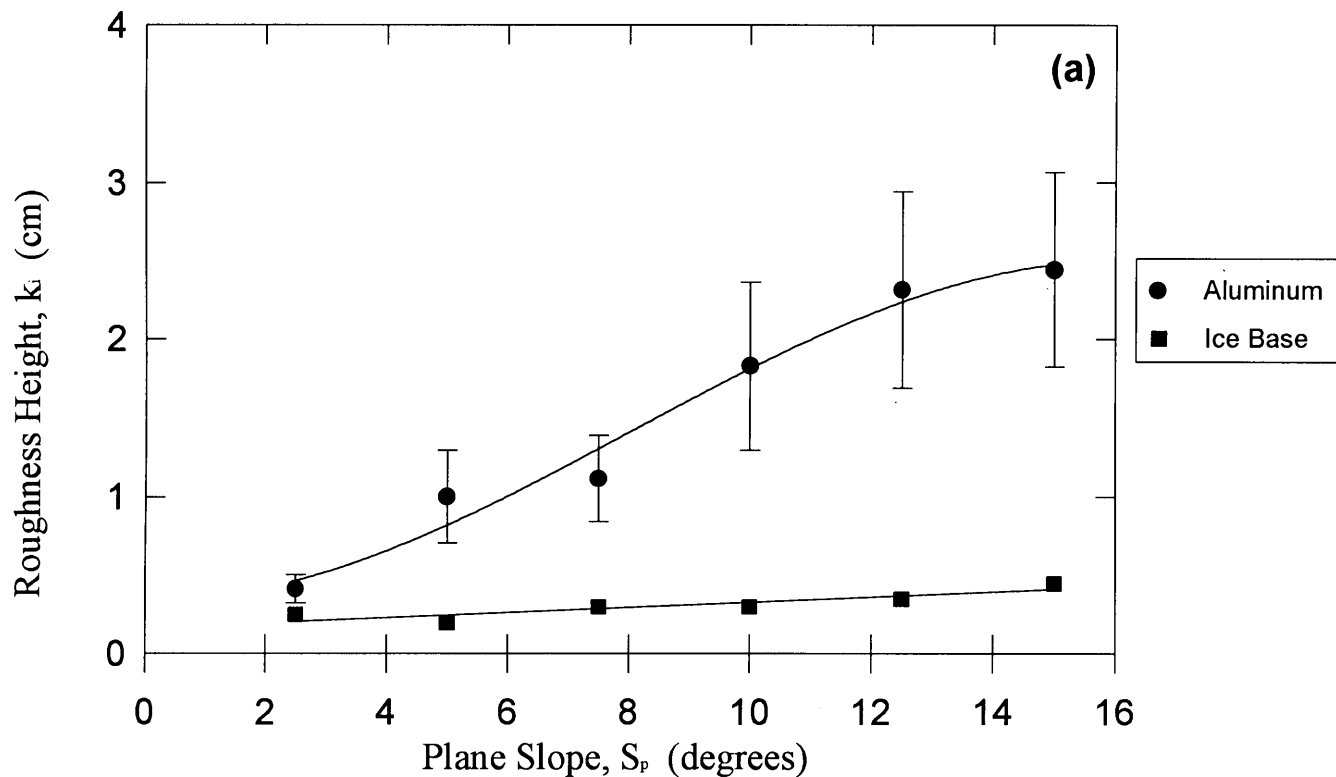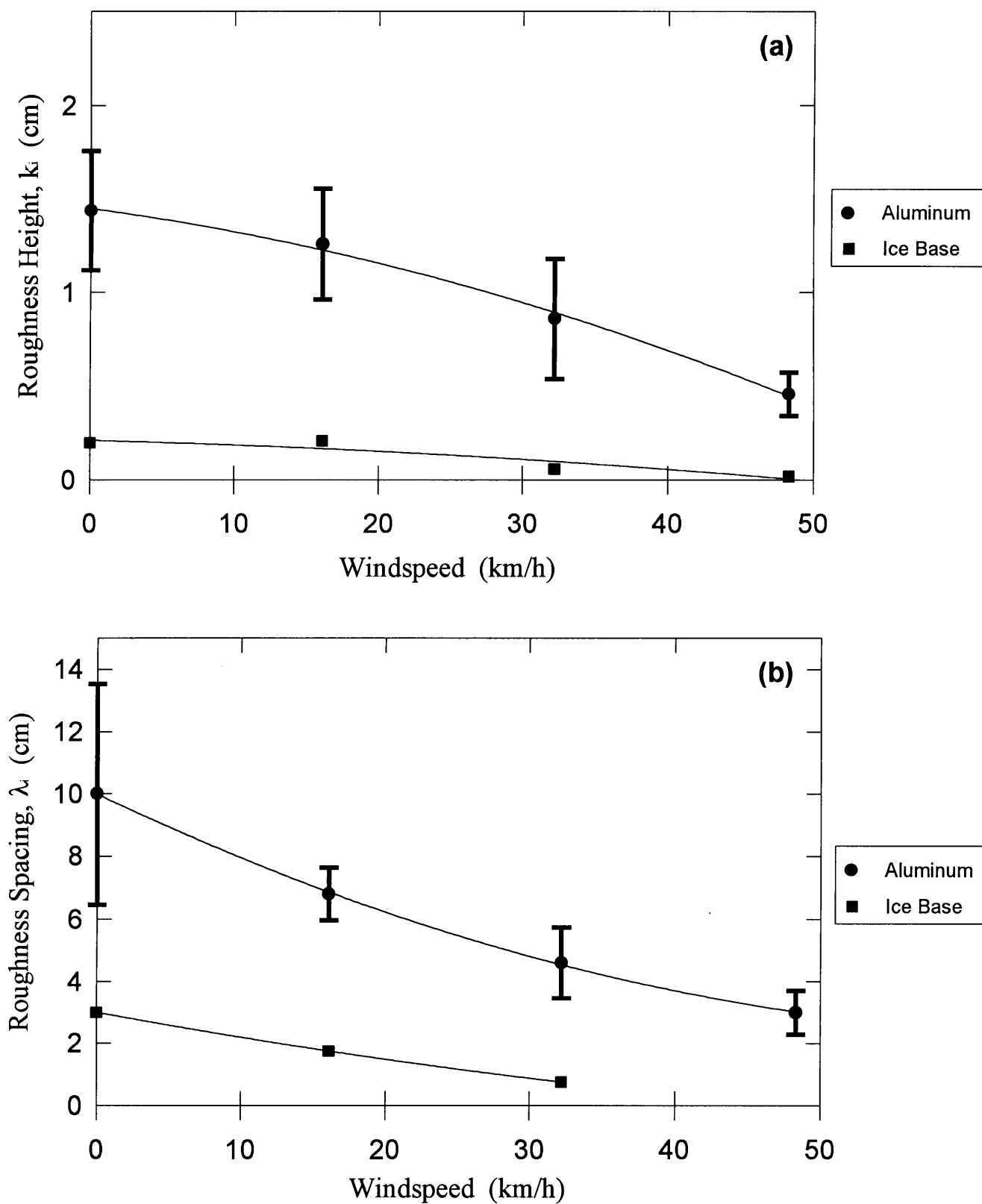
Figure 5.5 Effects of windspeed on icing roughness (plane slope = 8 degrees).

5.2   Formation and features of sheet-flow icings on a smooth ice surface

In contrast with ice formation on a wet aluminum surface, ice formation on the initially smooth ice was uniform and slushy. The aerial density of initial nucleation sites was much greater than for the wetted case. Also, the ice did not exhibit the damming and pooling seen in the cases for which the aluminum surface was wetted, nor did it display growth in the transverse and upstream directions.

Typical features for the cases with an initial ice cover over the aluminum plate were much less pronounced. The overall topology was much smoother and more uniform in appearance (shorter spacing and lower heights). Consequently, measuring roughness element heights and the distances between the roughness elements was much more difficult. Figure 5.6 is a photo showing the typical features of this type of icing. Note the marked contrast to Figure 5.2, as the flow and air temperature conditions were the same. The magnitude of roughness height and spacing was on the order of millimeters, whereas the same parameters measured centimeters in length for icings on the initially wet aluminum plate.

Plane slope and wind had much less of an effect on ice forming on the surfaces that were initially ice covered. Both the smooth and bumpy initial ice cover cases resulted in variations with slope and wind that were difficult to detect. It was difficult to accurately measure the roughness height and spacing with the current experimental apparatus. The ice did, however, appear to be smoother with increased windspeed, exhibiting decreased roughness height and spacing. Figures 4.4 and 4.5

indicate trends in roughness features. They should, however, be considered strictly qualitative, given the limitations mentioned above.
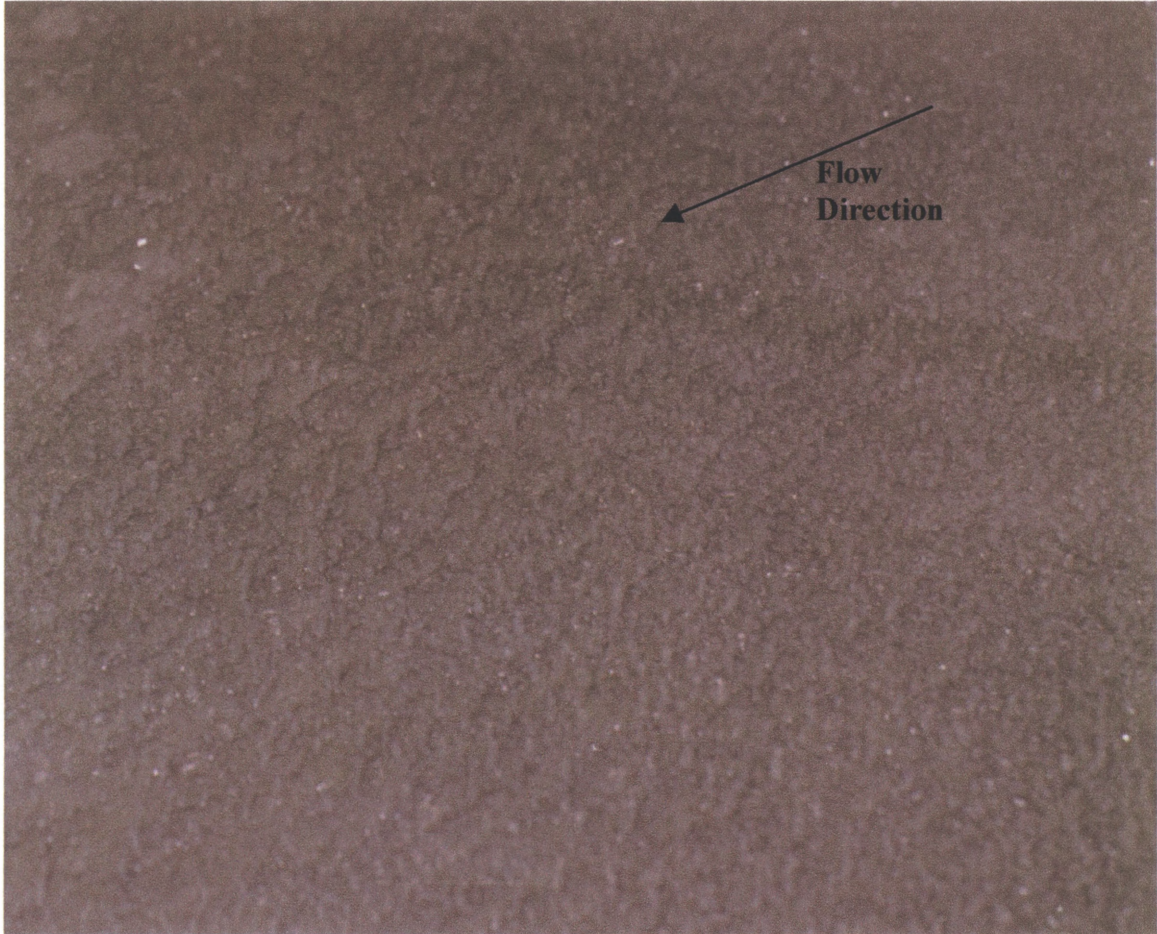
Figure 5.6   Typical features of icing forming on an ice surface.

5.3   Formation and features of sheet-flow icings on aluminum surface with ice bumps

Similar to the icings formed on the smooth-ice covered surface, icing formations on the aluminum surface with ice bumps was uniform and slushy. Indeed, icings formed under the two different initial conditions were qualitatively indistinguishable. Further study could be performed, varying the aerial density of the

ice bumps. The limiting case of infinite aerial density is the 100% ice covered case. The case of very low or zero density is representative of the bare aluminum experiments.

5.4   Formation and typical features of freezing rivulets

As the water flowed from the point source, it formed a single rivulet that propagated downstream. Surface tension and, relatively, the limited wetting nature of the water/aluminum interface dominated the rivulet flow. Plane slope and windspeed also affected the rate of rivulet propagation. The rivulet frequently stalled and re-started. Branching occurred at the rivulet front as well as at points upstream from the front. The rivulets meandered and often re-joined the main stem of the rivulet from which they branched.

Water in the rivulets initially froze at the frigid aluminum base. Water flow continued as a slushy layer of fine dendrites formed across the bottom of the rivulet. The bond with the aluminum plate was strong enough to not be scratched easily away by finger. In contrast, the slushy formation in the flowing section of the rivulet was easily dislodged. As time progressed, the bond to the base plane increased in strength and thickness, and the slushy dendrite growth increased in density. As ice growth increased in the rivulet, water welled from the rivulet, overcoming surface tension, and flowed over the frozen surface of the rivulet downstream. This caused the rivulets to widen over time, often joining with parallel rivulets or filling in dry voids created by meandering, branching, and re-joining.

Figures 5.7 and 5.8 illustrate how the rivulets propagate. Figures 5.7a-c comprise a series of photographs taken at two-minute intervals. A rivulet front is evident in Figure 5.7a at point 1. If the rivulet is traced back upstream, it is evident that it has branched off of a larger rivulet. The larger rivulet, observable in the lower portion of Figure 5.7a, shows a darker-colored portion. The darker portion is the initial rivulet formed, consisting of a strong bond to the base plane and a dense, slushy cross-section. Widening of the rivulet, out from the surface area covered by the initial rivulet, is also evident in this Figure. Two minutes later, in Figure 5.7b, the smaller rivulet has re-joined the larger, another small branching and re-joining has occurred, and more widening has taken place. Slushy dendrite growth can now be seen in the widened portion of the rivulets. In Figure 5.7c, further widening has caused most of the dry void space to be covered with water. The process continues with the overall effect of the rivulets joining and widening, ultimately encountering the lateral constraints of the test section.

Figure 5.8 illustrates similar formations as Figure 5.7 but provide a wider view of rivulet freezing. The photographs in Figure 5.8 were taken at two-minute intervals, beginning at three minutes after the start of the experimental run. As in Figure 5.7, meandering, branching, re-joining, and widening can be seen. The flow conditions and temperature are the same in Figures 5.7 and 5.8.

Photographs of typical features of rivulet icing are presented in Figure 5.9. Note the meandering, branching, and re-joining as discussed in the previous section.
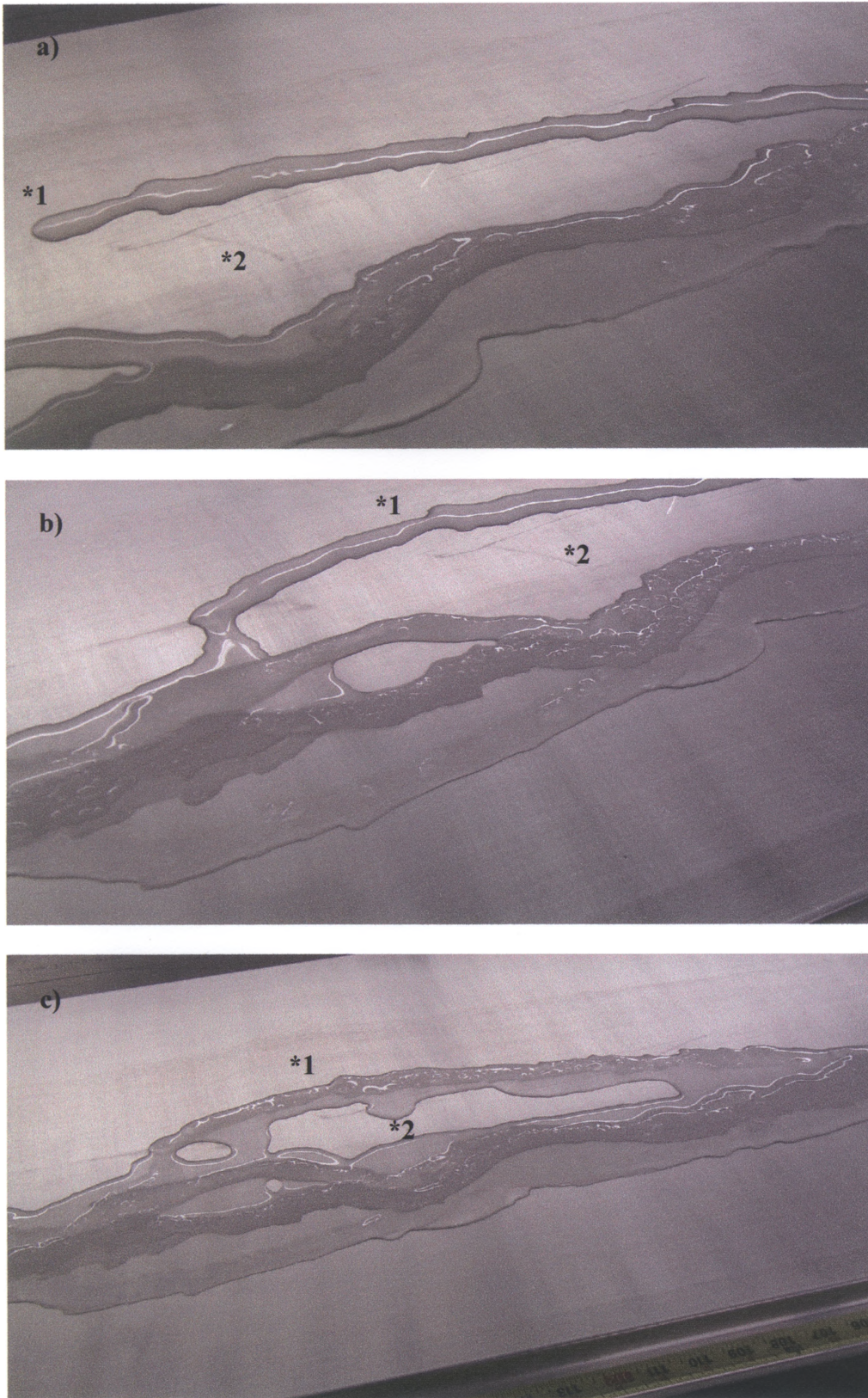
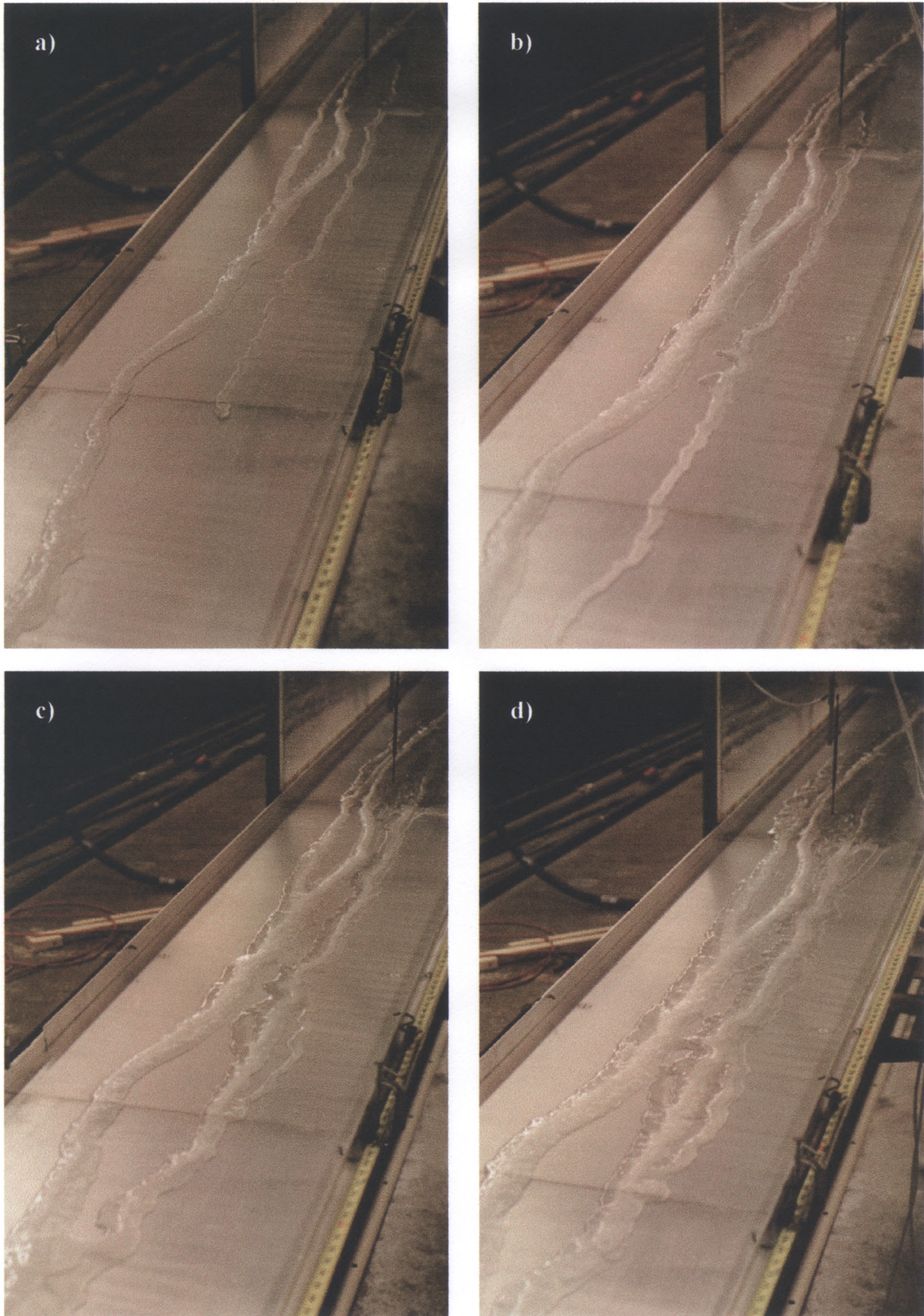Figure 5.7   Close-up views of a series of rivulet ice development.

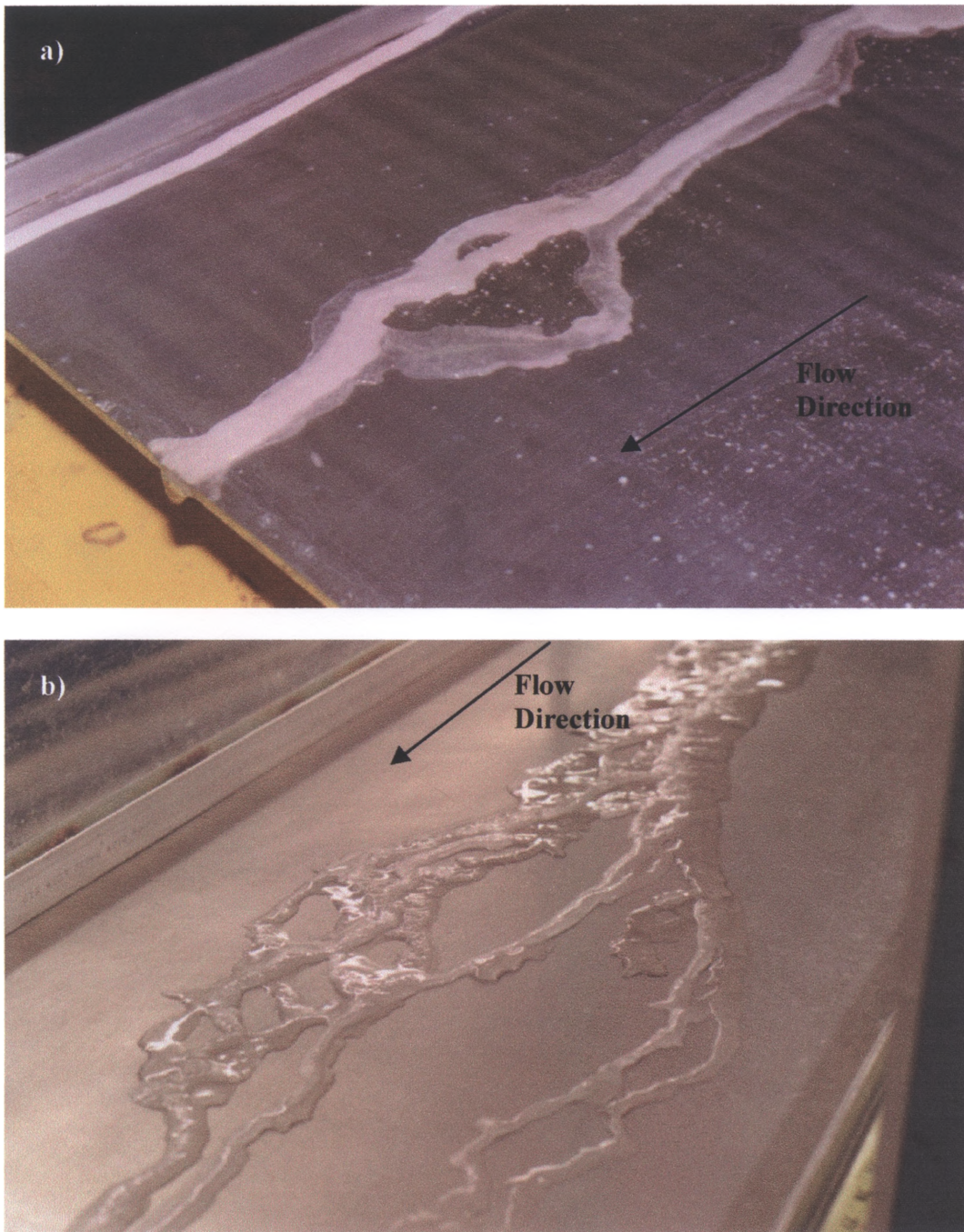Figure 5.8   Photographs of a series of rivulet ice development.

Figure 5.9   Typical features of rivulet icing.

Plane slope and windspeed significantly influence icing surface features and spread rates of freezing rivulets. The plots in Figure 5.10 show the average propagation distance of rivulet fronts versus time, for constant plane slopes. The three lines on each plot represent mean experimental values at three different windspeeds. The trends show that the rivulet front tends to travel faster when subject to lower windspeeds. This result is somewhat counter-intuitive. One might expect the higher windspeeds to drive the flow at a faster rate. In actuality, the increased windspeeds increased heat transfer and thinned the flow, resulting in a slower moving front, and an increase in the volume of liquid water changed to ice. Also, at higher windspeeds, the rivulets were much more likely to reach a length for which the volumetric rate of ice formation equaled the volumetric rate of water supplied to the icing, before going off of the end of the test section. This length is analogous to the equilibrium length of Schohl and Ettema (1986).

The plots in Figure 5.11 show the average propagation distance of rivulet fronts versus time, for constant windspeeds. The three lines on each plot represent mean experimental values at three different slopes. As one might anticipate, higher slopes are shown to result in increased rates of propagation.

Figures 5.12, 5.13, and 5.14 are plots showing individual experimental trials for the same conditions as in the average-value plots in Figures 5.10 and 5.11. The plots of the individual experimental trials show the trends discussed above, but also provide additional insight. For example, Figure 5.12a shows the rivulets stalling and re-starting. This was a common occurrence for the cases of low slope (1.5 degrees).

Higher plane slope resulted in less varied rivulet propagation (evident as smoother lines on the plots).

Table 1 gives the total discharge volume of liquid water for various plane slopes with all other parameters held constant. The water was collected at the downstream end of the test section, as shown in Figure 3.3. An increase in slope is shown to increase the amount of liquid water that arrives at the downstream end of the test section unfrozen. Discharge for higher windspeeds was zero, as the equilibrium length was realized.

The average time of propagation of rivulets to the end of the test section is given in Table 2. The rivulets reached an equilibrium length for all windspeeds greater than zero. The steeper the slope, the faster the rivulet front propagated to the end of the test section (6.3 m).

Table 1. Average total discharge for various slopes at t=10 min., windspeed = 0.

Plane Slope (degrees)	Discharge (liters)
1.5	0.22
3.0	0.31
4.5	0.38

Table 2. Average time of propagation to end of test section for windspeed = 0.

Plane Slope (degrees)	Time (seconds)
1.5	190
3.0	68
4.5	57

a) Average Rivulet Propagation for 1.5 deg. Slope

b) Average Rivulet Propagation for 3.0 deg. Slope

c) Average Rivulet Propagation for 4.5 deg. Slope
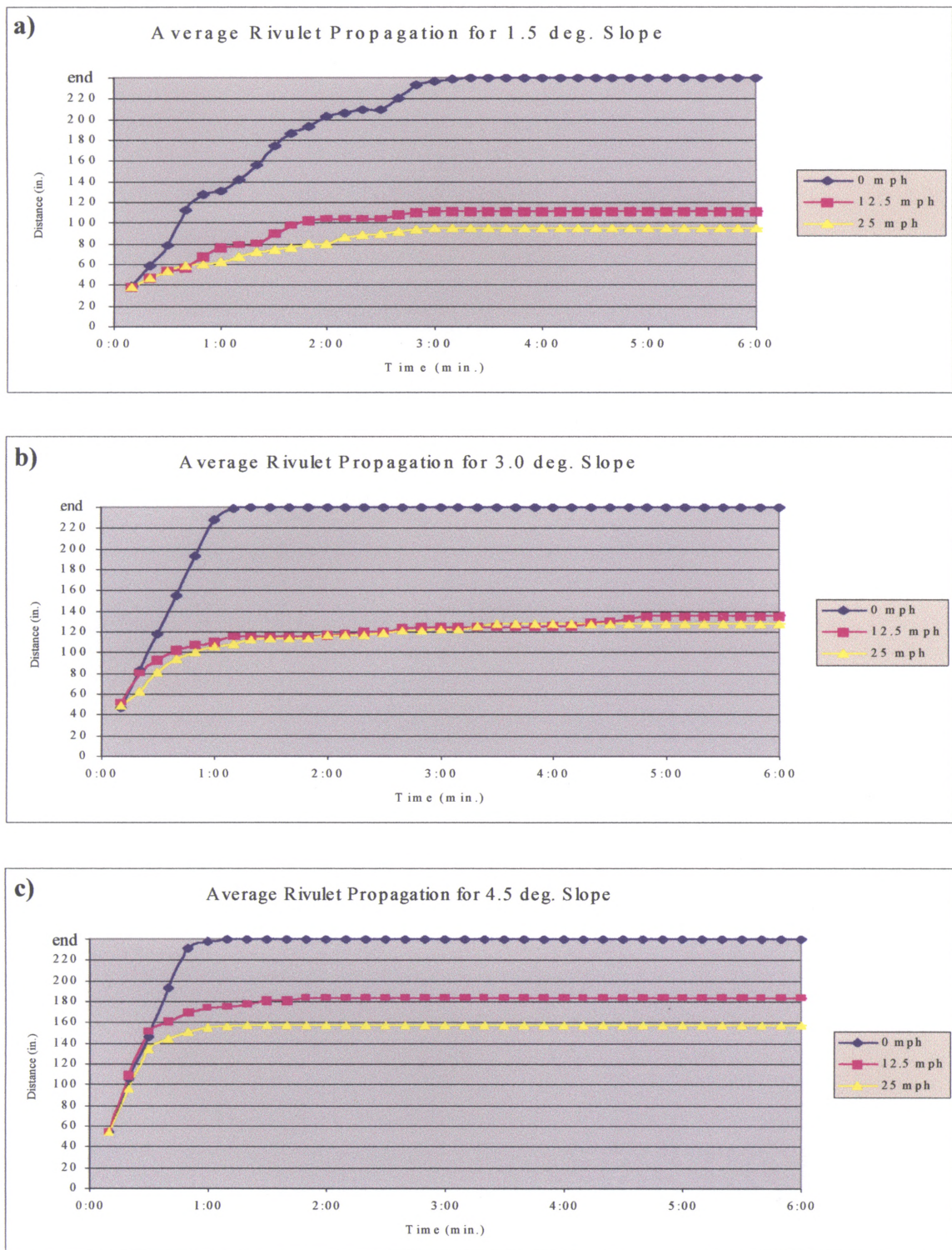
Figure 5.10   Average propagation of rivulet fronts for constant slope.

a)

Average Rivulet Propagation for 0 mph Windspeed

b)

Average Rivulet Propagation for 12.5 mph Windspeed

c)

Average Rivulet Propagation for 25 mph Windspeed

Figure 5.11   Average propagation of rivulet fronts for constant windspeed.

a)

Propagation of Rivulet Front for 1.5 deg. Slope and 0 mph Windspeed

b)

Propagation of Rivulet Front for 1.5 deg. Slope and 12.5 mph Windspeed

c)

Propagation of Rivulet Front for 1.5 deg. Slope and 25 mph Windspeed

Figure 5.12   Propagation of rivulet fronts for 1.5 degree Slope.

54
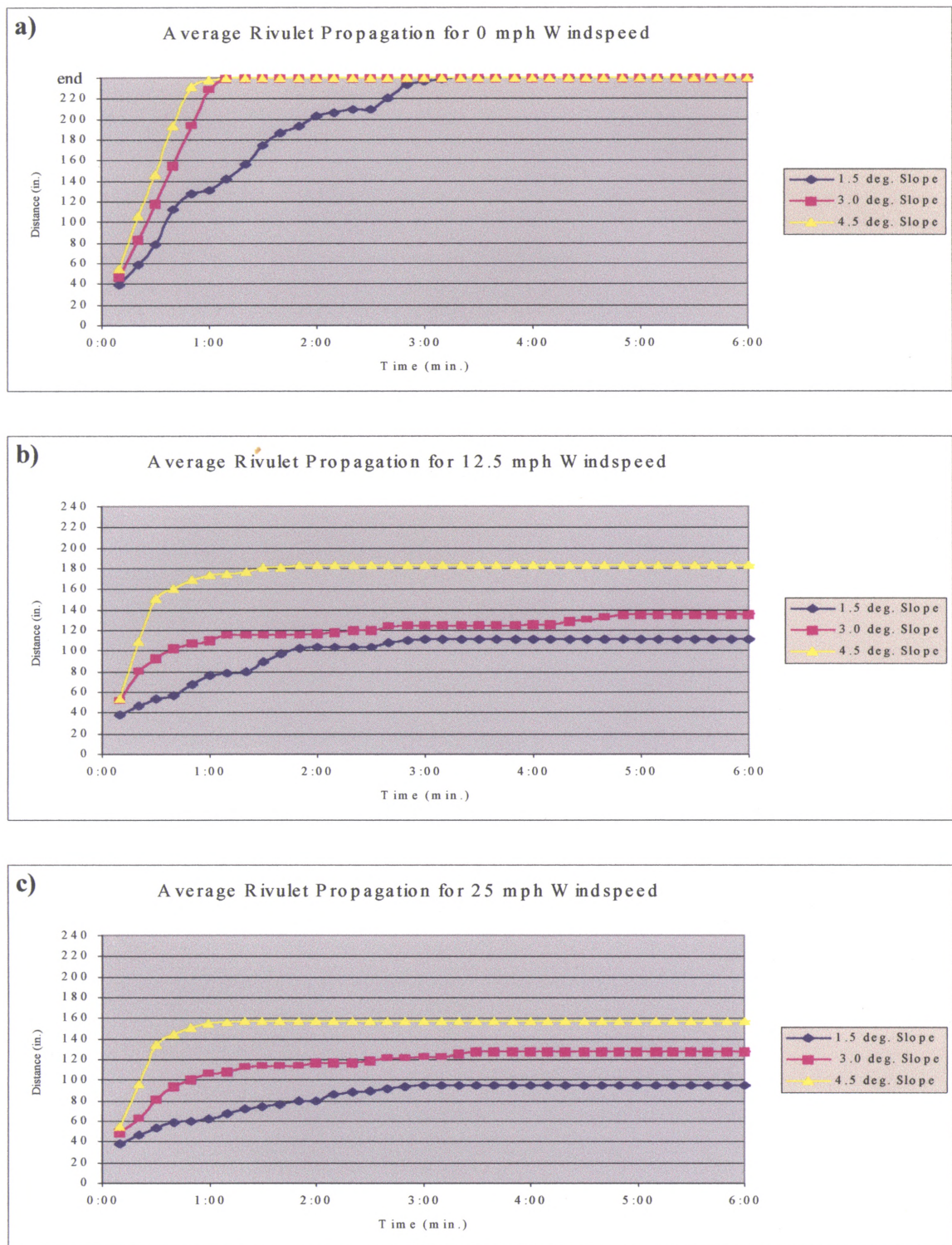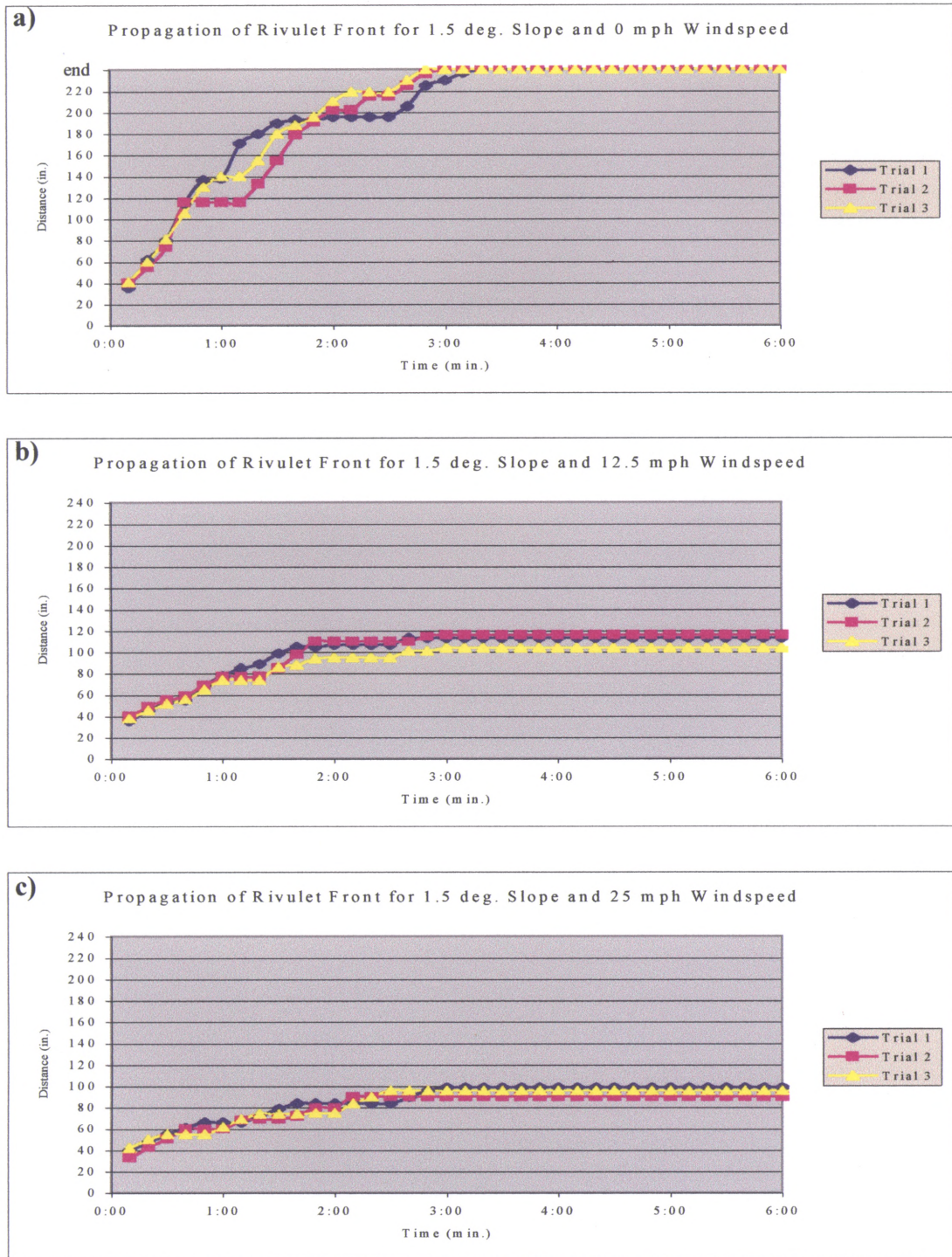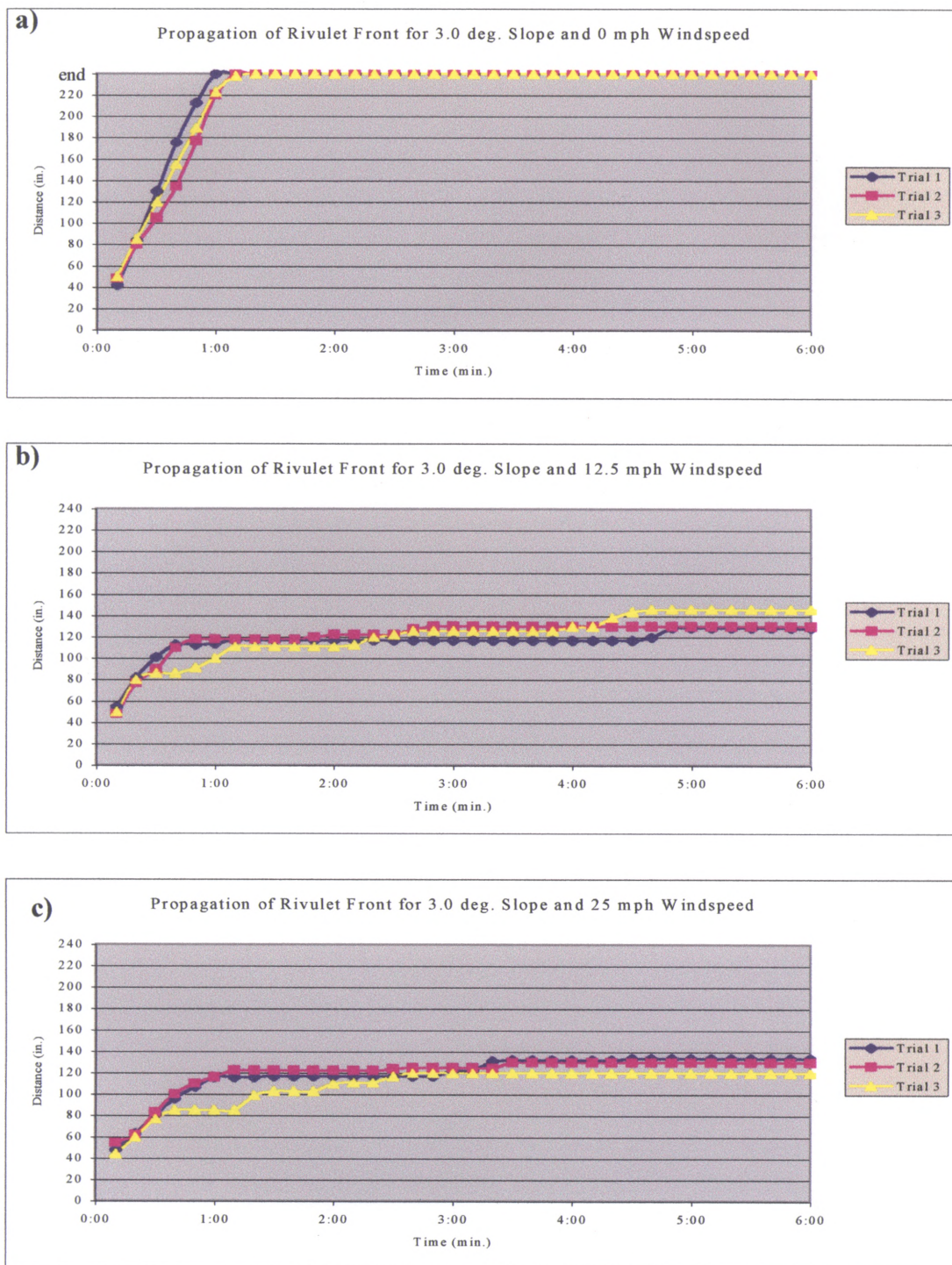

Figure 5.13   Propagation of rivulet fronts for 3.0 degree Slope.
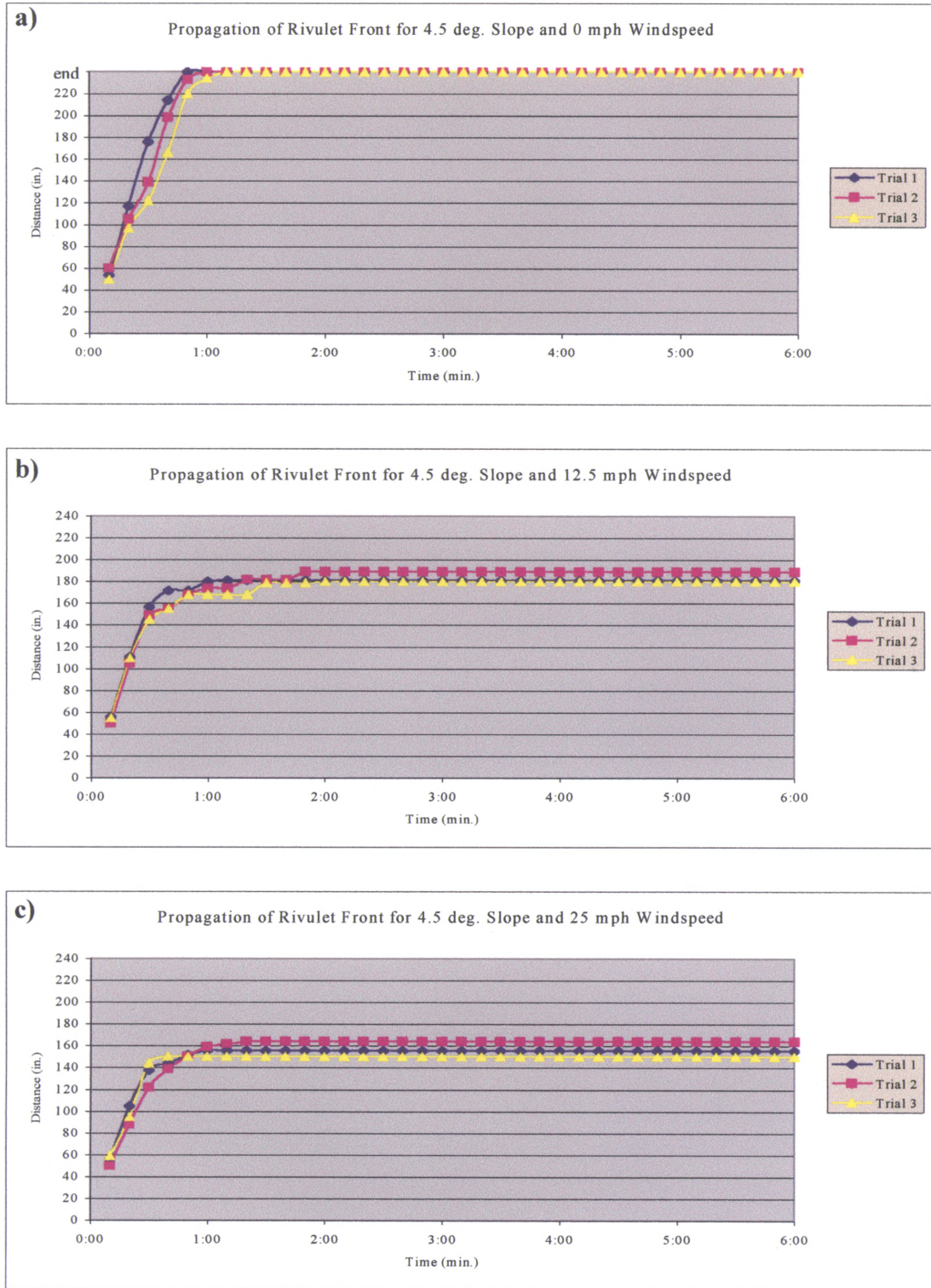
Figure 5.14   Propagation of rivulet fronts for 4.5 degree Slope.

Figure 5.15 presents plots of rivulet width versus time, for three windspeeds. The rivulets were measured at their widest point. Each data point represents the average value of 2 experimental runs. The base slope was fixed at 3.5 degrees. Higher windspeed resulted in rivulets that spread laterally at a faster rate. Wind drag resulted in thinner, wider rivulets, which froze more quickly, causing the water flow to spread even more. This result also could be derived from the plots, which show that the rivulets stalled at a shorter equilibrium length with increased windspeed. If the discharge is constant, and the equilibrium length is shorter, then the rivulet must widen laterally.
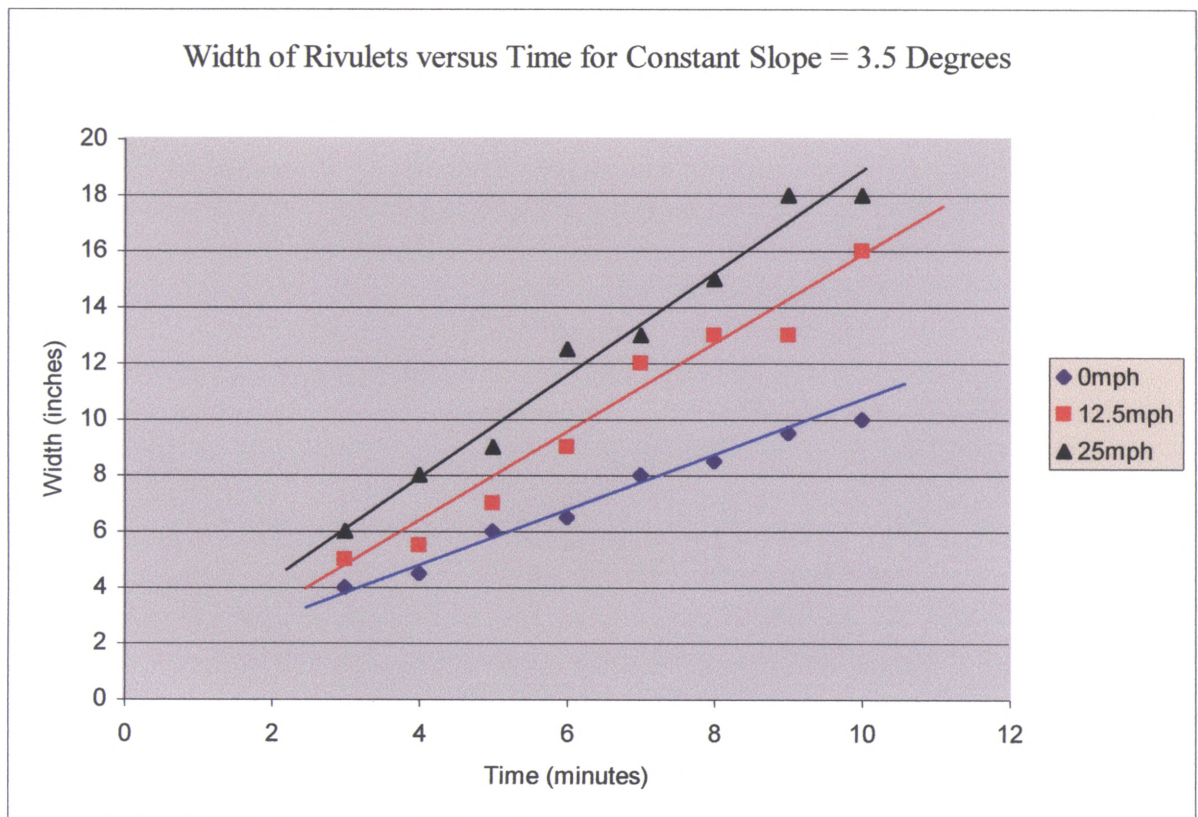

Figure 5.15   Width of rivulets versus time for constant slope and varying windspeed.

CHAPTER VI

CONCLUSIONS AND RECOMMENDATIONS

FOR FUTURE RESEARCH

6.1   Conclusions

The initial spreading and topologic features of icings vary significantly with the slope of the base plane on which icing forms, the rate of water supply, the water, air, and surface temperatures, the type of flow (sheet or rivulet), and the presence of wind.

1. Plane slope and wind speed significantly influence the surface features of icings formed on a wet aluminum base,

2. Icing roughness spacing and height decrease with increasing wind speed.

3. Roughness spacing decreases with increasing slope, but roughness height increases for the range of slope studied.

4. Roughness spacing and height of icings formed on an ice base are more uniform and at a smaller scale than for those formed on wetted aluminum.

5. Higher slopes and windspeeds result in smoother icings.

6. Rivulets are affected by variations in base slope and by the presence of wind.

7. The speed at which freezing rivulets propagate down-slope increases with increased slope, but decreases with increased windspeed due to thinning of the flow, increased heat transfer, and the subsequent higher rate of ice formation.

8. Consequently, rivulets reach a shorter equilibrium length at higher windspeeds.

6.2   Recommendations for further research

The icing windtunnel developed for this study is a useful facility for investigating icings formed from thin sheets or rivulets of water. However, further refinements could be made to the facility.   In particular, refining the system that controls the flow of water at prescribed temperatures would enable a more quantitative study of the icings investigated in the present study, as well as other, more complicated flows.   A more accurate method of measuring the important features of icing (i.e. roughness) would also be beneficial.

Additionally, considerable scope exists for the further investigation of more combinations of the dimensionless parameters in equation (5).   For example, the influence of base-plane roughness should be considered.   Also, freezing of rivulets should be investigated for the several regimes of rivulet flow (straight, sinuous, meandering, branching).

REFERENCES

1.   Akhtaruzzaman, A.K.M., Wang, C.K., and Lin, S.P., *Journal of Applied Mechanics*, Vol. 25, 1978, p.25.

2.   Al-Khalil, K.M., "Numerical Simulation of an Aircraft Anti-Icing System Incorporating a Rivulet Model for the Runback Water," Ph.D. Dissertation, Univ. of Toledo, Toledo, OH, 1990.

3.   Al-Khalil, K.M., Keith, T.G., and Dewitt, K.J., "Development of an Anti-Icing Runback Model," AIAA Paper 90-0759, Reno, NV, 1989.

4.   Al-Khalil, K.M., Keith, T.G., and Dewitt, K.J., "Further Development of an anti-Icing Runback Model," AIAA Paper 91-0266, 1991.

5.   Al-Khalil, K.M., Keith, T.G., Dewitt, K.J., Nathman, J.K., and Dietrich, D.A., "Thermal Analysis of Engine Inlet Anti-Icing Systems," *Journal of Propulsion and Power*, Vol. 6, No. 5, 1990, p.628.

6.   Anderson, D.A., Tannehill, J.C., and Pletcher R.H., *Computational Fluid Mechanics and Heat Transfer*, Hemisphere, New York, 1984, p.55.

7.   Ashton, G.D., *River and Lake Ice Engineering*, Water Resources Publications, Colorado, 1986.

8.   Benjamin, T.B., "Wave Formation in Laminar Flow Down an Inclined Plane," *Journal of Fluid Mechanics*, Vol. 2, 1957, p.554.

9.   Binnie, A.M., *Journal of Fluid Mechanics*, Vol. 2, 1957, p.551

10.   Gorycki, M.A., "Hydraulic Drag: a Meander-Initiating Mechanism," *Bulletin of the Geological Society of America*, Vol. 84, 1973, p.175.

11.   Goussis, D.A., and Kelly, R.E., *APS Bulletin* Vol. 30, 1985

12.   Goussis, D.A., and Kelly, R.E., *Phys. Fluids*, 1988

13. Hansman, R.J., and Turnock, S.R., "Investigation of Microphysical Factors which Influence Surface Roughness During Glaze Ice Accretion," 4th International Conference on Atmospheric Icing of Structures, Paris, France, 1988.

14. Hansman, R.J., and Turnock, S.R., "Investigation of Surface Water Behavior During Glaze Ice Accretion," *Journal of Aircraft*, Vol. 26, No. 2, 1989, p.140.

15. Hansman, R.J., Yamaguchi, K., Berkowitz, B., and Potapczuk, M., "Modeling of Surface Roughness Effects on Glaze Ice Accretion," AIAA Paper 89-0734, Reno, NV, Jan. 1989.

16. Hickox, C.E., *Phys Fluids*, Vol. 214, 1971, p.251

17. Hooper, A.P., *Phys. Fluids*, Vol. 28, 1985, p.1613

18. Joseph, D.D., Renardy, M., and Renardy, Y., *Journal of Fluid Mechanics*, Vol. 141, 1984, p.309.

19. Kao, T.W., *Phys. Fluids*, Vol. 8, 1965a, p.812.

20. Kao, T.W., *Phys. Fluids*, Vol. 8, 1965b, p.2190.

21. Kao, T.W., *Journal of Fluid Mechanics*, Vol. 33, 1968, p.561.

22. Lin, S.P., "Stability of Liquid Flow Down a Heated Inclined Plane," *Lett. Heat Mass Transfer*, 1975, p. 361

23. Lister, J.R., *Journal of Fluid Mechanics*, Vol. 175, 1987, p.413

24. Liu, J., Paul, J.D., and Gollub, J.P., "Measurements of the Primary Instabilities of Film Flows," *Journal of Fluid Mechanics*, Vol. 250, 1993, p.69.

25. Mizumura, K., "Meandering Water Rivulet," *Journal of Hydraulic Engineering*," ASCE, 1993 p. 1205.

26. Renardy, Y., *Phys. Fluids*, Vol. 30, 1987a, p.1627

27. Renardy, Y., *Phys. Fluids*, Vol. 30, 1987b, p.1638

28. Schmuki, P., and Laso, M., "On the Stability of Rivulet Flow," *Journal of Fluid Mechanics*, Vol. 215, 1990, p125.

29. Schohl, G. A., and Ettema, R., "Naled Ice growth," Report No. 297, Iowa Institute of Hydraulic Research, The University of Iowa, Iowa City, IA, 1986

30. Smith, M.C., "The Long Wave Instability in Heated or Cooled Inclined liquid Layers," *Journal of Fluid Mechanics*, Vol. 219, 1990, p.337.

31. Smith, M.K., and Davis, S.H., *Journal of Fluid Mechanics*, Vol. 121, 1982, p.187.

32. Than, P.T., Rosso, F., and Joseph, D.D., *International Journal of Engineering Science*, Vol. 40, 1987, p.70.

33. Towell, G.D., and Rothfeld, L.B., "Hydrodynamics of Rivulet Flow," *AIChE J.*, Vol. 12, No. 5, 1966, p.972.

34. Tsao, J.C., and Rothmayer, A.P., "A Mechanism for Ice Roughness Formation on an Airfoil Leading Edge, Contributing to Glaze Ice Accretion," AIAA paper 98-0485, 1998.

35. Yih, C.S., "Stability of Laminar Parallel Flow With a Free Surface," *Proceedings of 2nd U.S. National Congress on Applied Mechanics*, ASME, 1955, p.623.

36. Yih, C.S., "Stability of Liquid Flow Down an Inclined Plane," *Phys. Fluids*, 1963, p. 321.